Identification of a small molecule, Mebendazole, as a novel ethylene signaling activator reveals a role of ethylene signaling on the regulation of lateral root angles

Wenrong He 1, Ling Zhang 1, Min Cao 1, Neal Arakawa 3, Yao Xiao 4, Yingnan Hou 5, 6, Wolfgang Busch 1,2

1. Plant Molecular and Cellular Biology Laboratory, Salk Institute for Biological Studies, La Jolla, California, USA
2. Integrative Biology Laboratory, Salk Institute for Biological Studies, La Jolla, California, USA
3. Environmental and Complex Analysis Laboratory (ECAL), Department of Chemistry and Biochemistry, University of California, San Diego, La Jolla, USA
4. Department of Integrative Structural and Computational Biology, The Scripps Research Institute, La Jolla, California, USA
5. Department of Microbiology and Plant Pathology, Center for Plant Cell Biology, University of California, Riverside, California, USA
6. School of Agriculture and Biology, Shanghai Jiao Tong University, Shanghai, China

Corresponding author e-mail: Wolfgang Busch (wbusch@salk.edu)

Short title: Mebendazole inhibits CTR1 kinase activity

Material distribution footnote: The author responsible for distribution of materials integral to the findings presented in this article in accordance with the policy described in the Instructions for Authors is: Wolfgang Busch (wbusch@salk.edu)

Abstract

The lateral root angle or gravitropic set-point angle (GSA) is an important trait for root system architecture (RSA) that determines the radial expansion of the root system. The GSA therefore plays a crucial role in the ability of plants to access nutrients and water in the soil. Despite its importance, only few regulatory pathways and mechanisms that determine GSA are known, and these mostly relate to auxin and cytokinin pathways. Here, we report the identification of a small molecule that modulates GSA in *Arabidopsis thaliana* roots and acts via the activation of ethylene signaling. We uncover that this small molecule Mebendazole (MBZ) directly acts on the serine/threonine

protein kinase CTR1, which is a negative regulator of ethylene signaling. Our study not only reveals that the ethylene signaling pathway is essential for GSA regulation, but it also identifies a small molecular modulator of RSA and the first specific activator of ethylene signaling.

Introduction

The root systems of plants play a crucial role for plant survival and productivity as they are the key organs to capture water and nutrients from the soil. For efficiently foraging the soil for nutrients, the distribution of roots, root system architecture (RSA), is of enormous relevance. For instance, to enhance the capacity for root systems to efficiently uptake nitrogen and water, deeper roots are required, yet for improving the uptake of phosphate and other nutrients shallower soil layers have to be accessed by roots[2]. Deeper rooting is also associated with higher carbon permanence[3], a critical trait for soil carbon sequestration and the ability of plants to survive terminal droughts[4]. A key determinant of RSA is the lateral root angle or gravitropic set-point angle (GSA). Previous studies have shown that auxin plays a crucial role in regulating GSA[5-7]. Application of exogenous IAA or synthetic auxin leads to lateral root growth toward the vector of gravity thereby decreasing GSA[5,6]. Another phytohormone, cytokinin, was also found to be involved in the regulation of GSA. Application of cytokinin showed an anti-gravitropic effect and thereby increased GSA[8].

Ethylene is an ancient plant hormone whose signaling pathway is highly conserved and which has evolved in plants over 450 million years [9]. Ethylene is produced from the conversion of S-adenosyl-L-methionine (SAM) to 1-aminocy-clopropane-1-carboxylic acid (ACC) and then to ethylene, a step which is catalyzed by enzymes including ACC synthase (ACS) and ACC oxidase (ACO)[10,11]. When ethylene binds to its receptors (ETRs)[14-16], it inactivates a serine/threonine protein kinase, CONSTITUTIVE TRIPLE RESPONSE1(CTR1), which is the most upstream negative regulator of ethylene signaling[17]. In the absence of ethylene, CTR1 blocks ethylene downstream responses by phosphorylating the C-terminal of ETHYLENE-INSENSITIVE2 (EIN2), an ER–associated membrane protein that works as a positive regulator of ethylene signaling[18-

[20]. This leads to the degradation of EIN2-CEND by the Ub/26S proteasome[19-21]. When CTR1 is inactivated by ethylene binding to ETRs, EIN2-CEND is stabilized and moves into the nucleus to transduce the ethylene signal to downstream transcription factors, such as EIN3, EIN3 LIKE1 (EIL1)[22,23]and ETHYLENE RESPONSE FACTORs (ERFs)[24]. These transcription factors activate the downstream ethylene response. The ethylene pathway was found to play an important role in numerous of growth and developmental processes in the root, such as the inhibition of root elongation[17,25,26], induction of root hair growth[27], and inhibition the initiation of lateral roots (LRs)[28].

To identify potential regulators of GSA, we performed a chemical genetics screen and identified a small molecule, Mebendazole (MBZ), which dramatically increased GSA. Genetic analysis revealed that MBZ increased GSA through rapidly activating the ethylene signaling pathway. Both MBZ and ACC treatment induced ethylene signaling, which led to a modulation of lateral root angle. Further molecular and biochemistry studies showed that MBZ activates ethylene signaling by specifically targeting CTR1 and thereby blocking its kinase activity. This not only exposes MBZ as an efficient small molecular activator of ethylene signaling, but also that ethylene signaling plays an important role in regulating GSA.

Results

A small compound profoundly affects the lateral root gravitropic setpoint angle (GSA) **in Arabidopsis**

To identify small molecules that affect GSA, we screened chemicals for their ability to change GSA of young seedlings from a small molecular library with 2000 diverse generic chemicals (SP 2000)[29-31]. We found that treatment with Mebendazole (MBZ) (Supplementary Fig. 1a) led to a distinct increase of lateral root angles that caused lateral roots to grow in a more horizontal direction (Fig. 1a). The lateral root GSA of untreated two-week-old Arabidopsis seedlings was approx. 46°, and the GSA of lateral roots of seedlings grown on 1 μM MBZ plates was approx. 70° (Fig. 1a, b). While the lateral root angle was the most striking phenotype, at a much earlier developmental stage (one week after germination), seedlings on 1 μM MBZ displayed a decreased root

length (in average reduced by 37%) and an increased root hair initiation and elongation (Fig. 1c, d, Supplementary Fig. 1b). To test how quickly MBZ would affect root growth, we grew seedlings for 14 days on ½ MS medium with DMSO, then transferred them to ½ MS medium supplemented with 1 µM MBZ and acquired images every 10 minutes. All of the five measured lateral root tips started to grow at a more horizontal (less steep) angle within three hours of MBZ treatment (Fig. 1e upper panel, f). To test whether the action of MBZ was reversible, we germinated and grew seedlings on ½ MS for 5 days, and then transferred them to medium containing 1 µM MBZ for 12 days, thereby inducing lateral roots of MBZ treated seedlings to grow more horizontal. Finally, we transferred the seedlings back to control conditions and acquired images every 10 minutes. All 5 lateral root tips we measured started to grow at a distinctly steeper angle within four hours upon removal from MBZ (Fig. 1e bottom panel, f). These data showed that the treatment of Arabidopsis roots with MBZ changes lateral root angles within three hours and that this effect is fully reversible. In summary, we found that MBZ changes lateral root angles, and important RSA traits associated with the development of a shallow root system.

MBZ treatment specifically perturbs the ethylene pathway

Plant hormone pathways play a major role in determining RSA traits[32,33] and two plant hormones, auxin and cytokinin, have been shown to be involved in setting the GSA of lateral roots[5,6,8]. To unravel the mode of action of MBZ impact, we therefore first tested whether MBZ specifically acts on auxin or cytokinin. We compared root phenotypes of 8-day-old Arabidopsis seedlings grown on media plates with 1 µM MBZ and 10 nM IAA. We found that both treatments inhibited root elongation and enhanced root hair growth (Supplementary Fig. 2a, b). In addition, MBZ treatment induced *DR5-GFP V2* expression in 7-day-old roots (Supplementary Fig. 2c), suggesting auxin responses were induced by MBZ treatment. However, our data had shown that MBZ treatment distinctly increased lateral root angle, which is opposite to previous described auxin treated plants that showed a decrease in lateral root angle[5,6] and that could be reconfirmed under our conditions (Supplementary Fig. 2d, e). As auxin signaling can be regulated downstream of other signaling pathways, we looked at the timing of the onset

of the MBZ triggered auxin responses. Based on our time-lapse experiment we could see a change of GSA within one to four hours of MBZ treatment (Fig. 1e, f), we assumed that any relevant direct response to MBZ should be observable within this timeframe. However, no increased *DR5-GFP V2*[34] expression in roots treated with MBZ was observed within 3 hours compared to mock treatment (Supplementary Fig. 2f). To further exclude an involvement of the auxin response in the immediate response to MBZ, we measured changes in the orientation of microtubules, which is a hallmark response to auxin treatment[35]. The orientation of β-tubulin in roots significantly changed under 1 µM IAA but not upon 50 µM MBZ within 1 h (Supplementary Fig. 2g). Consistent with the results obtained from the *DR5-GFP V2* reporter and the microtubule reorientation experiments, expression of all marker genes of auxin signaling that we checked, including *IAA1*, *IAA29*, G*H3.2*, *GH3.3*, and *MAKR4* did not show any significant change upon MBZ treatment for 2h (Supplementary Fig. 2h). Together these data strongly suggested that the increased *DR5-GFP* V2 signal under long-term treatment is caused by an indirect regulation of auxin signaling or a feedback effect. We therefore concluded that MBZ was not directly acting upon the auxin pathway. We also tested whether the cytokinin response was elicited by MBZ treatment. For this, we first measured the expression of *ARR5*, which is one of the immediate-early cytokinin target genes. *ARR5* expression did not respond to MBZ treatment (Supplementary Fig. 2i) at 3h, 6h or 12 hours, suggesting that MBZ doesn't act upon the cytokinin pathway in the timeframe that we observe responses.

As we had not found evidence supporting the direct involvement of auxin and cytokinin in the immediate response to MBZ, we utilized a genome-scale expression profiling approach. For this, we performed an mRNA-seq experiment using roots of 14-days-old Arabidopsis grown on ½ MS media treated with 10 µM MBZ for 4 hours. The analysis revealed that 677 genes were induced compared to mock treatment (log2 fold change > 1) and 658 genes were repressed (log2 fold change < -1). A gene ontology (GO) analysis revealed that among the genes that MBZ impacted, genes involved in ethylene responses were strongly overrepresented. In particular, the GO process "negative regulation of ethylene-activated signaling pathway" (GO:0010105) was the most enriched process (21.03 fold enrichment, P-value: 6.07E-04) upon MBZ treatment (Fig.

2a), and the 4th most enriched GO process was “ethylene-activated signaling pathway” (GO:0009873) (10.83 fold enrichment, P-value:7.45E-05) (Fig. 2a). To explore this in more detail, we directly looked at the responses of genes involved in the ethylene hormone pathway. A major portion of these genes were differentially regulated by MBZ compared to mock treatment (Fig. 2a, b). To further investigate this in a gene annotation independent manner, we compared the set of genes that had responded to MBZ with published data of 4 h ethylene treatment[36]. Of the 1335 differentially expressed genes (DEGs) upon the 4 hours of MBZ treatment, 306 were overlapping with 1397 DEGs upon 4 hours of ethylene treatment (P-value: $p < 4.657e-143$) (Fig. 2c). More than 90% of these common DEGs retained the directionality of their expression change (i.e. genes upregulated by MBZ were also upregulated by ethylene treatment and vice versa) (Fig. 2d, e). Overall, these data indicated that MBZ acted on the ethylene pathway.

MBZ treatment mimics the effects of ethylene precursor ACC to induce ethylene responses

To investigate how MBZ treatment acts upon the ethylene response, we compared plant responses to MBZ and the ethylene precursor ACC. We focused on early responses within a two-hour timeframe, as we had observed the first changes in GSA of lateral roots to occur within three hours (Fig. 1f). The transcript level of *ERF1*, a marker gene for ethylene responses, was strongly induced by 10 µM MBZ as well as ACC treatment in root tissue after treatment for 2 hours (Fig. 3a). Moreover, EIN3, a major transcription factor involved in ethylene signaling, is also dramatically induced by both treatments according to the *35S-EIN3-GFP* protein level in *ein3eil1* background after 2 hours (Fig. 3b). These results suggested that MBZ has a similar activity to ACC for triggering ethylene responses. We therefore reasoned that if MBZ induced similar effects to ACC, we should observe similar growth regulatory responses.

The most characteristic response to ACC and ethylene treatment is the triple response[12] (Fig. 3c to e). Consistent with our hypothesis, 3-day-old etiolated seedlings treated with 10 µM MBZ showed a significant triple response phenotype (Fig. 3c to e). Using different doses of MBZ, we found that 2.5 µM of MBZ was sufficient to induce the triple response phenotype in a dark environment (Supplementary Fig. 3a to f). Consistent with

MBZ mimicking ethylene treatment, MBZ induced triple response was abolished in the ethylene insensitive mutants *ein2-5 and ein3eil1* (Supplementary Fig. 3d to f). Ethylene treatment inhibits root elongation mainly by repressing cell elongation[25,37]. We therefore measured the length of root cells of 4-day-old etiolated seedlings treated with 2.5 µM MBZ and 10 µM ACC, and found that mature cell size was reduced by both treatments (Fig. 3f to h). Altogether, our data strongly suggested that MBZ elicits its effects via the ethylene pathway.

MBZ actives ethylene signaling

Next, we set out to locate the target of MBZ in the ethylene pathway. First, we tested whether MBZ induces ethylene biosynthesis, or acts on the perception of ethylene, or on the ethylene signaling pathway. To test whether biosynthesis or perception of ethylene is affected, we utilized the *etr1* ethylene receptor mutants. Both strong alleles of *etr1*, *etr1-1* and *etr1-3*, still strongly responded to MBZ treatment (Fig. 4a to d). Moreover, 4-days-old etiolated seedlings of *etr1-3* treated with 2.5 µM MBZ showed the typical triple response phenotype, demonstrating that ethylene responses are triggered by MBZ even without the perception of ethylene. In contrast to the response to MBZ, *etr1-3* plants were completely insensitive to the treatment with 10 µM of ACC (Supplementary Fig. 3a to c). To further test the independence of MBZ action of ethylene biosynthesis, we measured ethylene production by GC-MS in 3-days-old etiolated Col-0 seedlings that were treated with 10 µM MBZ or ACC. Consistent with our hypothesis, ethylene production was dramatically induced by 10 µM ACC, but not detected in DMSO or 10 µM MBZ treated seedlings (Fig. 4e). Collectively, these results show that MBZ induces ethylene responses by targeting factors downstream of ethylene biosynthesis and perception.

To uncover which components of ethylene signaling are targeted by MBZ, we studied MBZ responses in key mutants of the ethylene signaling pathway. First, we checked the root inhibition phenotype in *ctr1-1*, *ein2-5, ein3eil1* mutants treated with MBZ and compared these responses to the Col-0 wildtype. *CTR1* is the first negative regulator of ethylene signaling, and *EIN2* acts downstream of *CTR1* to trigger ethylene signaling. *EIN3/EIL1* are core transcription factors of ethylene signaling, which work downstream

of *EIN2* (Fig. 5a). Roots of Col-0 were sensitive to 1.2 µM MBZ treatment and showed short roots and increased root hair development (Fig. 5b, c). However, *ctr1-1* mutants in which ethylene signaling is constitutively active, showed short roots and abundant root hairs without any treatment at an early stage. Due to this pronounced early-seedling phenotype, we could not confidently assess changes in response to MBZ. The root length of *ein2-5* and *ein3eil1* mutant plants was clearly not affected by MBZ treatment (Fig. 5b, c). We further measured lateral root angles at a later stage of development, which we had found to be a major effect of MBZ treatment. 2 to 3-weeks-old *ctr1-1*, *ein2-5*, and *ein3eil1* plants were all insensitive to MBZ with regards to lateral root angles (Fig. 5d to g). Interestingly, *ctr1-1* without MBZ treatment, showed an increased lateral root angle phenotype, which mimics MBZ treatment, suggesting that CTR1 might be the target of MBZ in ethylene signaling. Consistent with this hypothesis, *ein2-5* and *ein3eil1* didn't show a triple response upon MBZ treatment (Supplementary Fig. 3d to f). *ctr1-1* showed a constitutive triple response no matter whether it was treated with MBZ or not. Taken together our data showed that MBZ activates ethylene signaling by most likely interfering with CTR1 in ethylene signaling pathway.

MBZ is a potent inhibitor of CTR1 kinase activity

To pinpoint whether CTR1 and EIN2 is the target of MBZ, we capitalized on what is known about the activity of MBZ in mammalian systems. There, MBZ has been reported to be an inhibitor of the serine/threonine kinase *homo sapiens* (*hs*) MAPK14[38]. While EIN2 is a membrane protein with an N-terminal 12 transmembrane domain and a hydrophilic C-terminus[18], CTR1 is a serine/threonine protein kinase[17] that phosphorates EIN2 at the C-terminus[19-21]. Because both of *hs*MAPK14 and CTR1 are serine/threonine kinases, we hypothesized that CTR1 is the direct target of MBZ in plants. Since it was shown that there are 4 key amino acid residues of the catalytic site of *hs*MAPK14 that are relevant for MBZ binding[38], we first tested *in silico* whether these residues were conserved between *hs*MAPK14 and CTR1. For this, we aligned the amino-acid sequence of the Arabidopsis CTR1 and *hs*MAPK14 kinase domains (Fig 6a, Supplementary Fig. 4a, b). We found 3 (Lys578, Thr 625, and Asp 694) of the of 4 critical amino acid residues were conserved between the CTR1 kinase domain and that

of *hs*MAPK14 (Fig. 6a). The different key residue is Met 109 in *hs*MAPK14, which has been changed to Leu 628 in CTR1. Because both Met and Leu are amino acids with hydrophobic side chain and similar structure, it appeared possible that the replacement of Met by Leu in the CTR1 kinase domain does not significantly change the binding pocket structure for MBZ. We therefore hypothesized that the kinase domains of CTR1 and MAPK14 might have similar structures and function with regards to binding MBZ (Supplementary Fig. 4b).

To test this hypothesis, we first performed a molecular docking analysis using the published crystal structures of CTR1[39](PDB: 3PPZ) and MBZ (CHEMBL685). We found that MBZ is predicted to bind into the pocket of the CTR1 kinase domain (Fig. 6b) formed by the aforementioned key amino acids (Fig. 6a, b, Supplementary Fig. 4b). Overall, these analyses indicated that CTR1 could be the target of MBZ in Arabidopsis.

To further test this model, we expressed the recombinant kinase domains (KD) of CTR1 and MAPK4 (a MAPK protein in Arabidopsis with a highly similar amino acid sequence to *hs*MAPK14) (Supplementary Table 1, Supplementary Fig. 4c, d). We then confirmed the kinase inhibitory activity of MBZ through an *in vitro* phosphorylation assay via anti-Thiophosphate-Ester antibodies (Ref). MBZ inhibited the kinase activities of both CTR1-KD and MPK4 in a concentration dependent manner, but the inhibition for CTR1-KD was much more pronounced (Fig. 6c). In particular, 10 µM MBZ strongly inhibited the kinase activity of CTR1-KD, while 100 uM MBZ totally blocked its activity. This assay demonstrated that MBZ directly inhibited the kinase activity of CTR1-KD, strongly suggesting that CTR1 is a direct target of MBZ in Arabidopsis.

Taken together, our data support a model in which MBZ is a small molecular inhibitor of the CTR1 kinase activity and thereby triggers the ethylene signaling pathway by permitting EIN2C translocation into the nucleus, which in turn triggers ethylene downstream responses (Figure 7).

Discussion

Our chemical genetic screen led to the identification of MBZ as a potent inhibitor of the kinase activity of CTR1, which is a negative modulator of the ethylene signaling pathway (Fig. 7). MBZ therefore is an activator of ethylene signaling, and to our

knowledge is the first specific small molecule that acts as a regulator of ethylene signaling. While most of the effects of MBZ are related to its activation of ethylene signaling, our RNA profiling indicated additional effects of MBZ. Consistently, treatment with high concentration of MBZ or long-term treatment with it, led to strongly inhibited plant growth and development, including a disrupted root apical meristem and morphological changes of leaves. These phenotypes have not been observed upon ethylene treatment (Supplementary Fig. 5 a, b), raising the possibility that MBZ may have other targets in plants. MAPK4 has the highest amino acid sequence similarity to the human MBZ target *hs*MAPK14 (Supplementary Table. 1). However, compared to CTR1, the effect of MBZ on MAPK4 kinase activity was much less pronounced (Fig. 6 c), consistent with the lack of conservation of key amino acids relevant for MBZ binding (Supplementary Fig. 4c). Another explanation for the observed effects of MBZ that go beyond observed ethylene effects, might be that continuous activation of ethylene signaling via CTR1 might have more complicated or compounded effects than are elicited by external ethylene or ACC treatment (Supplementary Fig. 5c). Support for this comes from the *ctr1-1* mutant, which is dwarfed and shows aberration in leaf forms and thereby displays much stronger phenotypes than elicited with ACC or ethylene treatment[17] (Fig. 5b, d, Supplementary Fig. 5c).

One of the most intriguing effects of MBZ on the plant is its potent ability to change GSA. This suggests that ethylene signaling is involved in the regulation of the gravitropic setpoint angle in lateral roots. While ACC treatment had a weak but distinct effect on root angle and displayed concentration-dependent effects when applying a large range of concentrations (Supplementary Fig. 5c). it could not entirely mimic the effects of MBZ treatment in increasing lateral root angle. Since MBZ acts directly on ethylene signaling and ACC needs to be converted into ethylene in plant, it could be expected a number of downstream processes such as transport, cell-type specific permeability and conversion rates of ACC can lead to different outcomes. Moreover, ACC was recently found to be a signaling molecule to regulate pollen tube attraction, which is independent of ethylene pathway[40]. Strong direct evidence for the impact of ethylene signaling in regulating lateral root setpoint angle is provided by the RSA phenotype of the *ctr1-1* mutant. In

ctr1-1, ethylene signaling is constitutively activated and leads to an increased lateral root angle (Fig. 5d, e). One reason why the role of ethylene in the regulation of lateral root angles hasn''t been recognized so far, might be that it reduces lateral root formation by itself[28] making the study of lateral root angles more difficult. Our study strongly suggests that it will be worthwhile to explore the role of ethylene in root gravitropism and RSA. Since ethylene signaling is a widely conserved process in land plants, exploring the ability of MBZ or genetic perturbation of the ethylene pathway to change RSA in crop species might be highly worthwhile for RSA engineering.

Methods

Plant material and growth conditions.

Arabidopsis mutants and transgenic lines used in this study are in the Col-0 background if not mentioned otherwise. *etr1-1*(CS237) and *etr1-3*(CS3070) were ordered from ABRC, *ctr1-1* (Kieber, 1993) *ein2-5* (Alonso,1999), *ein3-1eil1-1* (Alonso, 2003), *ein3eil135S: EIN3-GFP* (He, 2011) were lab stock. *UBQ10p:TUB6-GFP* [41], *35S:DR5v2:3xGFP-NLS* [34] (Gift from Weijers lab, Col-Ultrecht background). Plants were grown in a walk-in growth chamber in long day conditions (16/8h) at 21°C, 50 uM light intensity, 60% humidity. During night time, temperature was decreased to 15°C.

Small Molecule Library and Screen Information

The SP2000 small molecule library was received from the University of California, Riverside. The library was screened at a concentration of 50 ~ 100 µM in 200 µL of liquid MS media. After being grown in the liquid media for 7 days, seedlings were transferred to vertical plates to grow for another 2 days. The root phenotypes were acquired by CCD flatbed scanners. After candidates were picked, a second round of screen by gradient concentration of candidate small molecules from 1 µM to 100 µM on vertical plates was performed to confirm the phenotype and optimal concentration.

Chemical Solutions

The stock solutions for preparing media for the plant experiments were Mebendazole (10 mM) in DMSO, ACC (10 mM) in dH2O, IAA (1 mM) in ethanol.

Root phenotyping

Root phenotype images on plates were acquired with CCD flatbed scanners (EPSON). Root lengths and lateral root angles were measured using Fiji (http://fiji.sc/Fiji).

Time lapse of lateral root angle phenotyping

14 d old seedling on DMSO plate or 19 d old seedling on mebendazole plate were transferred to DMSO or 1 µM mebendazole plates as described. Root phenotype images of these plates were acquired by CCD vertical scanners (EPSON) every 10 mins over a period of 24 hours using the tool described[43]. Root length and lateral root angles were measured using Fiji (http://fiji.sc/Fiji).

mRNA-seq analysis

14 d old seedlings on DMSO plates were transferred to ½ MS liquid plates with DMSO or 10 µM mebendazole treatment for 4 h, root tissues were collected for RNA extraction and RNA-seq.

a. Read alignment

The TAIR10 genome file and annotation file were obtained from the Arabidopsis Information resource web site (http://www.arabidopsis.org)[44]. The An aligner, called the Splice Transcripts Alignments to Reference (STAR) version 2.7.0a[45], was used to align short reads in the FASTQ files.

b. **Differential expression analysis**

Differential expression of genes between treatments and control was determined using the R package, *edgeR* (version 3.36.0)[46]. The *CPM* (counts per million) function from *edgeR* was used to normalize the counts and differentially expressed genes (DEGs) were identified using *glmLRT* function from edgeR. A false discovery rate (FDR < 0.05) and |log2FC| > 1 were used as the criterial values for identification of up-regulated and down-regulated DEGs.

C. Analysis of published Ethylene RNA-Seq

The fastq-dump utility from the Short Read Archive (SRA) Toolkit (v2.6.3) (https://github.com/ncbi/sra-tools) was used to download transcriptome libraries (SRA accession IDs: SRR648276, SRR648275, SRR648274, SRR648300, SRR648299, and SRR648298) from SRA database (https://www.ncbi.nlm.nih.gov/sra)[47]. The color space sequencing data were converted to base-space sequencing data using Perl script 'csfq2fq.pl' (https://gist.github.com/pcantalupo/9c30709fe802c96ea2b3). The converted FASTQ files were aligned and analyzed using above methods.

Measurement of ethylene production.

100 seeds of Col-0 were planted and sealed in a screw-top 20 mL vial containing 10 mL ½ MS medium supplemented with DMSO (control), 10 µM mebendazole, and 10 µM ACC treatments (4 replicates). These vials were incubated at 22 °C for 3 days under dark environment. 500-1000 µL sample of the headspace gas was sampled with an autosampler (TriPlus RSH, Thermo Scientific) and injected into a gas chromatograph (Trace 1310 GC, Thermo Scientific) that was equipped with a HP-PLOTQ column (30 mm, 320 µm, 20 µm) and a mass spectrometer (TSQ8000 Evo MS, Thermo Scientific), scanning from 25-27.5 m/z. Separations were carried out at 35°C using He as the carrier gas. The area of the ethylene peak (RT: 4 min) was integrated using Thermo Xcalibur Qual Browser. A calibration curve was generated by varying the injection volume (100 µL, 250 µL, 500 µL, and 1000 µL) of a 10 ppm ethylene standard (in nitrogen), and sample results are expressed as concentrations calculated from linear regression of calibration samples.

Microscopy

A Zeiss 710 confocal microscope with 20x, 40x, and 63x objectives were used to detect GFP and propidium iodide (PI) fluorescence. A Keyence BZ-X810 microscope with a 20x objective was used to detect bright field images and GFP fluorescence in fig. 3**b**, Sfig. 1**b** right panel, Sfig. 2**c**, **f**.

Computational Docking and Molecular Modeling

The AutoDock Vina and Chimera software were used to dock mebendazole (CHEMBL685) into crystal structure of CTR1 (PDB: 3PPZ) and MAPK14 (PDB: 6SFO). Figures for those structures were visualized and generated by Chimera and Pymol.

Protein purification

The CTR1 Kinase domain (540 aa-821 aa) (CTR1-KD) and MAPK4 were cloned into a pET28a. Proteins were expressed in Rosetta™ 2(DE3)pLysS Competent Cells. Cultures were incubated at 37 °C (OD 600: 0.7 to 0.9) and induced by adding 0.4 mM isopropylthioβ-D-galactoside (IPTG) at 20 °C for 22 h, 200 rpm. Cells were harvested and resuspended in lysis buffer (50 mM pH 7.5 Tris-HCl, 1mM EDTA, 100 mM NaCl, 20% glycerol, EDTA-free protease inhibitor cocktail, 10 mM imidazole). followed by sonication and centrifugation (13,000 × g × 20 min). The His-tagged proteins were first purified using QIAGEN Ni-NTA Agarose. The elute from Ni-NTA was collected and further purified by FPLC using superdex 200 Increase 10/300 column[48]. The fractions corresponding to single peak from FPLC were combined, and concentrated to a desired volume. Protein purity was verified by coomassie blue gel staining. Protein concentration was measured by their absorbance at 280 nm.

***In vitro* kinase assay with non-radioactive ATP-γ-S**

The *in vitro* kinase assay followed the previous published method[49]. 100 ng purified recombinant CTR1-KD or 1 μg MPK4 was mixed with 2 μg Myelin Basic Protein (MBP, a common kinase substrate, Sigma Cat. M1891) and 1 mM ATPyS in kinase reaction buffer (10 mM HEPES pH 7.4, 150 mM NaCl, 10 mM MgCl2, 1xRoche Complete Protease Inhibitor mixture) and different concentration of MBZ at room temperature and vortexed for 1 hour. The reactions were terminated by 20 mM EDTA, and the proteins were alkylated by 1.5 uL of 50 mM PNBM (CAYMAN CHEMICAL CO, Cat. 21456-1) at room temperature and vortexed for 2 hours. The reactions were terminated by denaturing in NuPAGE™ LDS Sample Buffer and 1x NuPAGE™ Sample Reducing Agent (Invitrogen™). Samples were subjected to SDS-PAGE. The phosphorylation status of MBP, CTR1-KD and MPK4 were analyzed by western blot using Recombinant Anti-Thiophosphate ester antibody (Abcam, Cat. Ab92570, 1:5000) .

Statistical analysis

A two-sided Student's t-test was used for comparisons of two conditions. The comparison of meristem length, mature cell length, root length, GSA between multiple treatments or genotypes was performed by One-way ANOVA and *post hoc* Tukey testing. Detailed information was prepared in figure legends. Statistical significance of overlap between DEGs from MBZ treatment and ethylene treatment was assessed by hypergeometric distribution test.

Accession Numbers

Sequence data from this article can be found in the Arabidopsis Genome Initiative or GenBank/EMBL databases or Uniprot databases under the following accession numbers: *ERF1* (AT3G23240), *ETR1* (AT1G66340), *CTR1* (AT5g03730), *EIN2* (AT5G03280), *EIN3* (AT3g20770), *EIL1* (AT2G27050), *MAPK4* (AT4G01370), and *hsMAPK14* (HGNC:6876). Accession numbers of protein and chemicals structures used in the molecular modeling in Figure 6 are as follows: CTR1 (PDB: 3PPZ), MAPK14 (PDB: 6SFO) and MBZ (CHEMBL685).

Supplemental Data

Sfig. 1| MBZ treatment affects root growth and development.

Sfig. 2| MBZ treatment does not directly regulate auxin or cytokinin pathways.

Sfig. 3| Etiolated seedling phenotypes in mutants of the ethylene pathway.

Sfig. 4| Alignment of CTR1-KD in Arabidopsis and MAPK14 in human.

Sfig. 5| High concentrations or long-term treatment of MBZ induce phenotypes that go beyond ethylene induced effects.

S table 1. The list of blast hits in Arabidopsis using the MAPK14_human sequence as BLASTP.

Acknowledgements

The research was supported by start-up funds from the Salk Institute for Biological Studies and funds from the Harnessing Plants Initiative to WB, a Salk Women &

Science Special Award and a Pioneer Fund Postdoctoral Scholar Award to WH. We are grateful to Dr. Glenn R. Hicks and Dr. Natasha Raikhel for sharing the SP2000 small molecule library. We also thank Dr. Joseph R. Ecker and Dr. Joanne Chory for critical discussions. We thank the Next Generation Sequencing Core of Salk institute for NGS Library preparation & sequencing. We also thank Matthieu Platre, Nicole Gibbs, Anna Malolepszy, Björn Willige and Travis Lee for fruitful discussions and suggestions.

Author contributions

Wenrong He and Wolfgang Busch conceived the project and the experiments. Wenrong He performed the SP2000 library screen and analysis with help from Yingnan Hou. Wenrong He performed the phenotyping, qPCR, microscope, alignment, docking, protein purification, kinase activity assay and provided the tissue for mRNA-seq. Ling Zhang conducted the mRNA-seq analysis. Wenrong He and Ling Zhang performed the statistical analysis. Wenrong He conducted the Gene ontology and heatmap analysis of mRNA-seq. Min Cao provided the protocol and suggestions for kinase activity assay. Neal Arakawa performed the GC test. Yao Xiao performed the FPLC. Wenrong He and Wolfgang Busch wrote the manuscript with input from all authors. Wolfgang Busch provided supervision, guidance and advice on the project, the experiments, and the analysis of the results.

References

Allen, J. J. *et al.* (2007) A semisynthetic epitope for kinase substrates. *Nat Methods* **4**, 511-516, doi:10.1038/nmeth1048

Alonso, J. M., Hirayama, T., Roman, G., Nourizadeh, S. & Ecker, J. R. (1999) EIN2, a bifunctional transducer of ethylene and stress responses in Arabidopsis. *Science* **284**, 2148-2152, doi:10.1126/science.284.5423.2148

An, F. *et al.* (2010) Ethylene-induced stabilization of ETHYLENE INSENSITIVE3 and EIN3-LIKE1 is mediated by proteasomal degradation of EIN3 binding F-box 1 and 2 that requires EIN2 in Arabidopsis. *Plant Cell* **22**, 2384-2401, doi:10.1105/tpc.110.076588

Ariey-Bonnet, J. *et al.* (2020) In silico molecular target prediction unveils mebendazole as a potent MAPK14 inhibitor. *Mol Oncol* **14**, 3083-3099, doi:10.1002/1878-0261.12810

Berardini, T. Z. *et al.* (2015) The Arabidopsis information resource: Making and mining the "gold standard" annotated reference plant genome. *Genesis* **53**, 474-485, doi:10.1002/dvg.22877

Chang, C., Kwok, S. F., Bleecker, A. B. & Meyerowitz, E. M. (1993) Arabidopsis ethylene-response gene ETR1: similarity of product to two-component regulators. *Science* **262**, 539-544, doi:10.1126/science.8211181

Chang, K. N. *et al.* (2013) Temporal transcriptional response to ethylene gas drives growth hormone cross-regulation in Arabidopsis. *Elife* **2**, e00675, doi:10.7554/eLife.00675

Chao, Q. *et al.* (1997) Activation of the ethylene gas response pathway in Arabidopsis by the nuclear protein ETHYLENE-INSENSITIVE3 and related proteins. *Cell* **89**, 1133-1144, doi:10.1016/s0092-8674(00)80300-1

Chen, X. *et al.* (2014) Inhibition of cell expansion by rapid ABP1-mediated auxin effect on microtubules. *Nature* **516**, 90-93, doi:10.1038/nature13889

De Cnodder, T., Vissenberg, K., Van Der Straeten, D. & Verbelen, J. P. (2005) Regulation of cell length in the Arabidopsis thaliana root by the ethylene precursor 1-aminocyclopropane- 1-carboxylic acid: a matter of apoplastic reactions. *New Phytol* **168**, 541-550, doi:10.1111/j.1469-8137.2005.01540.x

Dobin, A. *et al.* (2013) STAR: ultrafast universal RNA-seq aligner. *Bioinformatics* **29**, 15-21, doi:10.1093/bioinformatics/bts635

Feng, Y. *et al.* (2017) Ethylene promotes root hair growth through coordinated EIN3/EIL1 and RHD6/RSL1 activity in Arabidopsis. *Proc Natl Acad Sci U S A* **114**, 13834-13839, doi:10.1073/pnas.1711723115

Guo, H. & Ecker, J. R. (2004) The ethylene signaling pathway: new insights. *Curr Opin Plant Biol* **7**, 40-49, doi:10.1016/j.pbi.2003.11.011

Guzman, P. & Ecker, J. R. (1990) Exploiting the triple response of Arabidopsis to identify ethylene-related mutants. *Plant Cell* **2**, 513-523, doi:10.1105/tpc.2.6.513

He, W. *et al.* (2011) A small-molecule screen identifies L-kynurenine as a competitive inhibitor of TAA1/TAR activity in ethylene-directed auxin biosynthesis and root growth in Arabidopsis. *Plant Cell* **23**, 3944-3960, doi:10.1105/tpc.111.089029

Hua, J. *et al.* (1998) EIN4 and ERS2 are members of the putative ethylene receptor gene family in Arabidopsis. *Plant Cell* **10**, 1321-1332, doi:10.1105/tpc.10.8.1321

Ju, C. *et al.* (2012) CTR1 phosphorylates the central regulator EIN2 to control ethylene hormone signaling from the ER membrane to the nucleus in Arabidopsis. *Proc Natl Acad Sci U S A* **109**, 19486-19491, doi:10.1073/pnas.1214848109

Ju, C. *et al.* (2015) Conservation of ethylene as a plant hormone over 450 million years of evolution. *Nat Plants* **1**, 14004, doi:10.1038/nplants.2014.4

Kieber, J. J., Rothenberg, M., Roman, G., Feldmann, K. A. & Ecker, J. (1993) R. CTR1, a negative regulator of the ethylene response pathway in Arabidopsis, encodes a member of the raf family of protein kinases. *Cell* **72**, 427-441, doi:10.1016/0092-8674(93)90119-b

Le, J., Vandenbussche, F., Van Der Straeten, D. & Verbelen, J. P. (2001) In the early response of Arabidopsis roots to ethylene, cell elongation is up- and down-regulated and uncoupled from differentiation. *Plant Physiol* **125**, 519-522, doi:10.1104/pp.125.2.519

Leinonen, R., Sugawara, H., Shumway, M. (2011) & International Nucleotide Sequence Database, C. The sequence read archive. *Nucleic Acids Res* **39**, D19-21, doi:10.1093/nar/gkq1019

Li, B. *et al.* (2019) GSNOR provides plant tolerance to iron toxicity via preventing iron-dependent nitrosative and oxidative cytotoxicity. *Nat Commun* **10**, 3896, doi:10.1038/s41467-019-11892-5

Liao, C. Y. *et al.* (2015) Reporters for sensitive and quantitative measurement of auxin response. *Nat Methods* **12**, 207-210, 202 p following 210, doi:10.1038/nmeth.3279

Lynch, J. P. (2021). Harnessing root architecture to address global challenges. *Plant J*, doi:10.1111/tpj.15560

Lynch, J. P. (2019). Root phenotypes for improved nutrient capture: an underexploited opportunity for global agriculture. *New Phytol* **223**, 548-564, doi:10.1111/nph.15738

Mayerhofer, H., Mueller-Dieckmann, C. & Mueller-Dieckmann, J. (2011) Cloning, expression, purification and preliminary X-ray analysis of the protein kinase domain of constitutive triple response 1 (CTR1) from Arabidopsis thaliana. *Acta Crystallogr Sect F Struct Biol Cryst Commun* **67**, 117-120, doi:10.1107/S1744309110047640

Mayerhofer, H., Panneerselvam, S. & Mueller-Dieckmann, J. (2012) Protein kinase domain of CTR1 from Arabidopsis thaliana promotes ethylene receptor cross talk. *J Mol Biol* **415**, 768-779, doi:10.1016/j.jmb.2011.11.046

Mou, W. *et al.* (2020) Ethylene-independent signaling by the ethylene precursor ACC in Arabidopsis ovular pollen tube attraction. *Nat Commun* **11**, 4082, doi:10.1038/s41467-020-17819-9

Muller, M. & Munne-Bosch, S. (2015) Ethylene Response Factors: A Key Regulatory Hub in Hormone and Stress Signaling. *Plant Physiol* **169**, 32-41, doi:10.1104/pp.15.00677

Nakamura, M., Naoi, K., Shoji, T. & Hashimoto, T. (2004) Low concentrations of propyzamide and oryzalin alter microtubule dynamics in Arabidopsis epidermal cells. *Plant Cell Physiol* **45**, 1330-1334, doi:10.1093/pcp/pch300

Negi, S., Ivanchenko, M. G. & Muday, G. K. (2008) Ethylene regulates lateral root formation and auxin transport in Arabidopsis thaliana. *Plant J* **55**, 175-187, doi:10.1111/j.1365-313X.2008.03495.x

Ogura, T. *et al.* (2019) Root System Depth in Arabidopsis Is Shaped by EXOCYST70A3 via the Dynamic Modulation of Auxin Transport. *Cell* **178**, 400-412 e416, doi:10.1016/j.cell.2019.06.021

Ogura, T., Goeschl, C. & Busch, W. (2022) A Multiplexed, Time-Resolved Assay of Root Gravitropic Bending on Agar Plates. *Methods Mol Biol* **2368**, 61-70, doi:10.1007/978-1-0716-1677-2_4

Pattyn, J., Vaughan-Hirsch, J. & Van de Poel, B. (2021) The regulation of ethylene biosynthesis: a complex multilevel control circuitry. *New Phytol* **229**, 770-782, doi:10.1111/nph.16873

Poirier, V., Roumet, C. & Munson, A. D. (2018). The root of the matter: Linking root traits and soil organic matter stabilization processes. *Soil Biology and Biochemistry* **120**, 246-259, doi:https://doi.org/10.1016/j.soilbio.2018.02.016

Qiao, H. *et al.* (2012) Processing and subcellular trafficking of ER-tethered EIN2 control response to ethylene gas. *Science* **338**, 390-393, doi:10.1126/science.1225974

Ristova, D., Giovannetti, M., Metesch, K. & Busch, W. (2018) Natural genetic variation shapes root system responses to phytohormones in Arabidopsis. *Plant J* **96**, 468-481, doi:10.1111/tpj.14034

Robinson, M. D., McCarthy, D. J. & Smyth, G. K. (2010) edgeR: a Bioconductor package for differential expression analysis of digital gene expression data. *Bioinformatics* **26**, 139-140, doi:10.1093/bioinformatics/btp616

Rosquete, M. R. *et al.* (2013).An auxin transport mechanism restricts positive orthogravitropism in lateral roots. *Curr Biol* **23**, 817-822, doi:10.1016/j.cub.2013.03.064

Roychoudhry, S., Del Bianco, M., Kieffer, M. & Kepinski, S. (2013). Auxin controls gravitropic setpoint angle in higher plant lateral branches. *Curr Biol* **23**, 1497-1504, doi:10.1016/j.cub.2013.06.034

Sakai, H. *et al.* ETR2 is an ETR1-like gene involved in ethylene signaling in Arabidopsis (1998) *Proc Natl Acad Sci U S A* **95**, 5812-5817, doi:10.1073/pnas.95.10.5812

Sun, X. *et al.* (2017) Pyrazinamide and derivatives block ethylene biosynthesis by inhibiting ACC oxidase. *Nat Commun* **8**, 15758, doi:10.1038/ncomms15758

Uga, Y. *et al.* (2013).Control of root system architecture by DEEPER ROOTING 1 increases rice yield under drought conditions. *Nat Genet* **45**, 1097-1102, doi:10.1038/ng.2725

Vaseva, II *et al.* (2018) The plant hormone ethylene restricts Arabidopsis growth via the epidermis. *Proc Natl Acad Sci U S A* **115**, E4130-E4139, doi:10.1073/pnas.1717649115

Waidmann, S. *et al.* (2019) Cytokinin functions as an asymmetric and anti-gravitropic signal in lateral roots. *Nat Commun* **10**, 3540, doi:10.1038/s41467-019-11483-4

Wen, X. *et al.* (2012) Activation of ethylene signaling is mediated by nuclear translocation of the cleaved EIN2 carboxyl terminus. *Cell Res* **22**, 1613-1616, doi:10.1038/cr.2012.145

Xiao, G. & Zhang, Y. (2020). Adaptive Growth: Shaping Auxin-Mediated Root System Architecture. *Trends Plant Sci* **25**, 121-123, doi:10.1016/j.tplants.2019.12.001

Yang, S F & Hoffman, N. E. 1984) Ethylene Biosynthesis and its Regulation in Higher Plants. *Annual Review of Plant Physiology* **35**, 155-189, doi:10.1146/annurev.pp.35.060184.001103

Zhu, Y. *et al.* (2019) A phenotype-directed chemical screen identifies ponalrestat as an inhibitor of the plant flavin monooxygenase YUCCA in auxin biosynthesis. *J Biol Chem* **294**, 19923-19933, doi:10.1074/jbc.RA119.010480

Figure legends

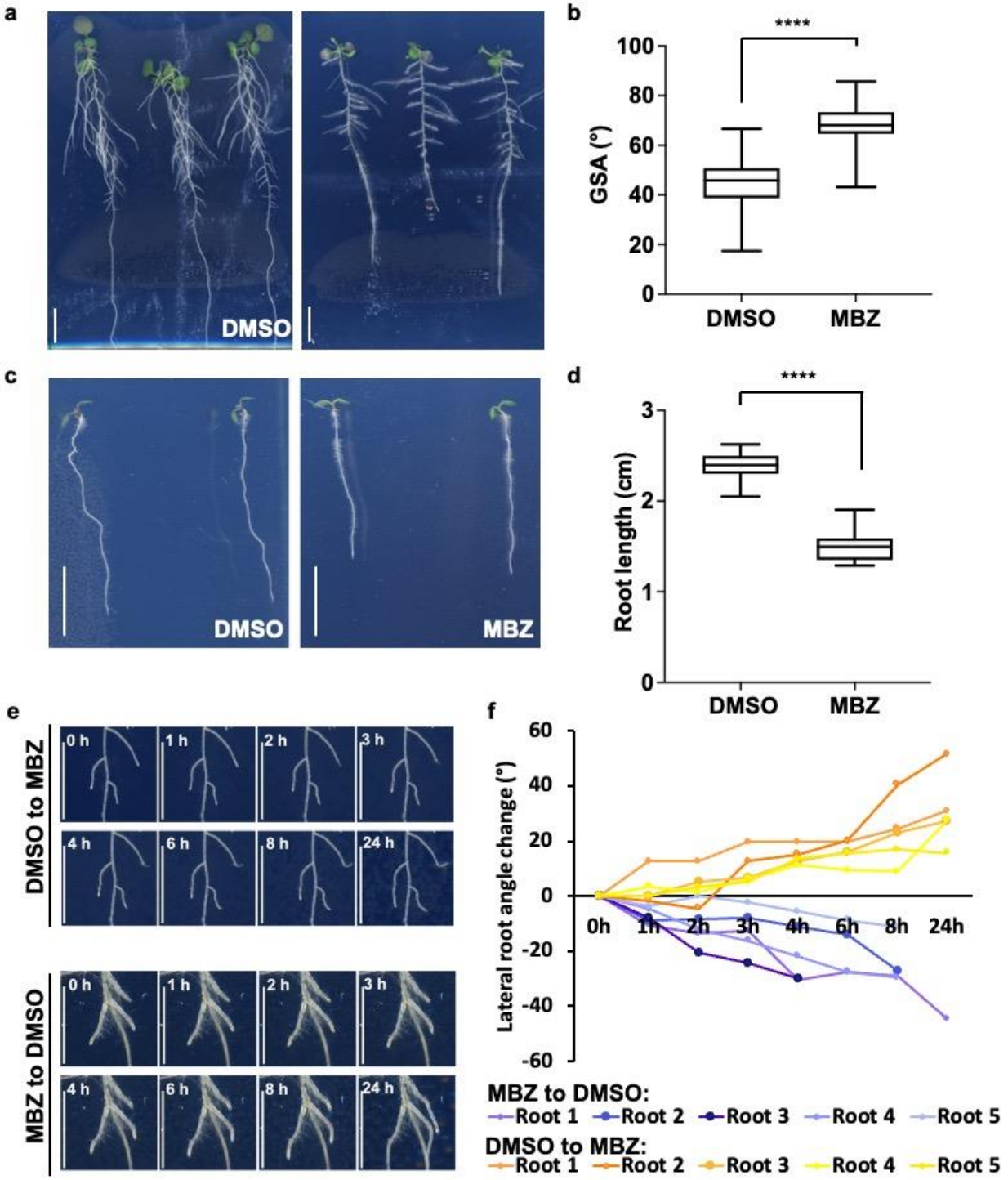

Fig.1 | MBZ treatment perturbs root system architecture (RSA). a, 14d seedlings of Arabidopsis grown on DMSO and MBZ (1 µM) plates. **b**, Quantification of GSA in (**a**). 15 LRs per seedling on DMSO plates, 12 LRs per seedling on MBZ plates, and 6 seedlings for each condition were used. Unpaired, two-tailed Student's t-tests was used for

statistical analysis. **** $p < 0.0001$. **c**, 5d seedlings on DMSO and MBZ (1 µM) plates. **d**, Quantification of primary root length (cm) in (**b**). 15-20 seedlings for each treatment were used. **** $p < 0.0001$. **e**, 12d (upper panel) Arabidopsis seedlings on DMSO plates were transferred to MBZ (1 µM) plates, and 17d (bottom panel) seedlings on MBZ (1 µM) plates were transferred to DMSO plates, followed by continuous scanning for 24 h. **f**, Changes of lateral root angle after plate transfer from DMSO to MBZ (red and yellow lines) or MBZ to DMSO (blue, purple lines) compared to timepoint 0. (Scale bar: **a**, **c**, **g**, 1 cm; **e**, 5 mm.). Boxplots: Whiskers: min/max values; hinges: 25th to 75th percentile; mid-line: median.

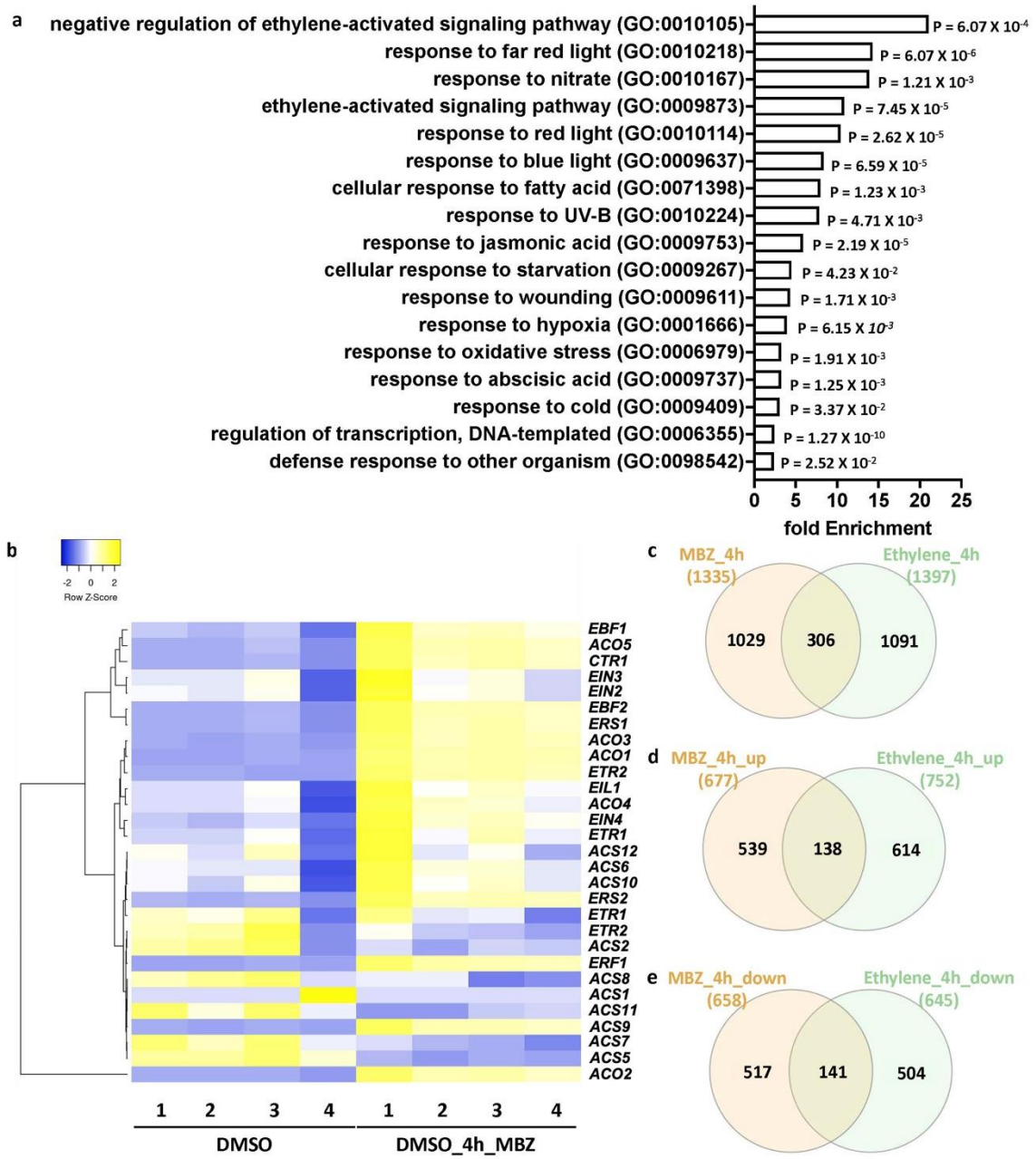

Fig. 2 | MBZ treatment regulates the ethylene pathway. **a**, Gene ontology (GO) analysis upregulated genes (log2 fold change > 1) upon MBZ treatment. **b**, Heatmap of genes involved in the ethylene pathway, which were regulated by MBZ treatment. **c-e**, Venn diagrams showing differentially expressed genes (abs(log2) fold change > 1) in 4h MBZ treatment and 4h ethylene treatment. All genes (**c**), upregulated genes (**d**), downregulated genes (**e**).

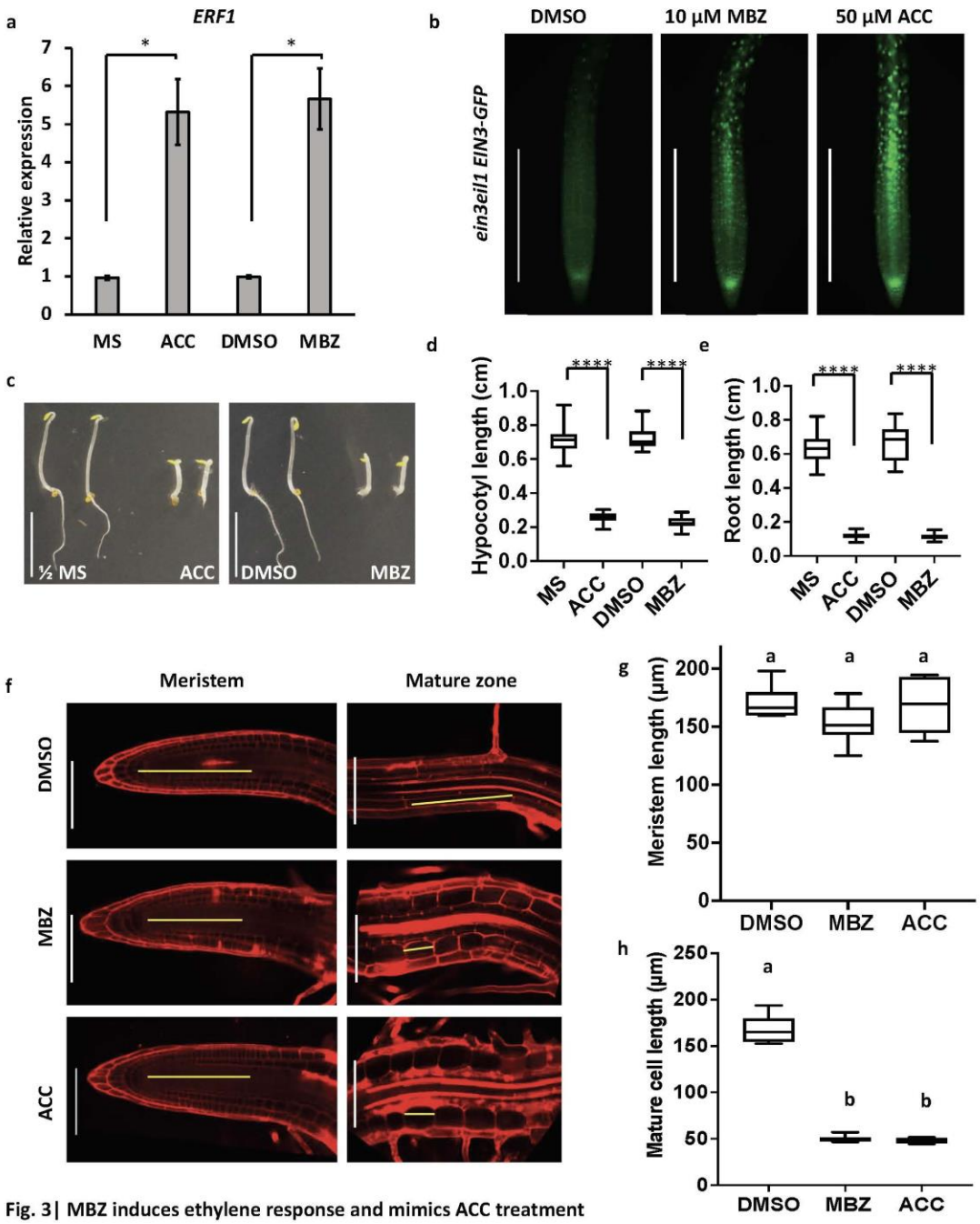

Fig. 3| MBZ induces ethylene response and mimics ACC treatment

Fig. 3 | MBZ induces ethylene responses and mimics ACC treatment. **a**, Quantification of ERF1 expression upon MS, 50 µM ACC, DMSO, and 10 µM MBZ treatments for 2 h in the Col-0. Unpaired, two-tailed Student's t-tests. * $p < 0.05$. Bars represent mean values ± s.d. from two technical replicates. Similar results were obtained from three biological replicates of the experiment. **b**, GFP fluorescence in root

tips of *ein3 eil1* 35S:EIN3-GFP treated for 2 hours with DMSO, 10 µM MBZ, 50 µM ACC. 6-10 seedlings were observed for each treatment. **c**, 4d etiolated seedlings grown on MS, 10 µM ACC, DMSO, 10 µM MBZ plates. 20 seedlings were observed for each treatment. **d-e**, Quantification of hypocotyl length (**d**) and root length (**e**) of seedlings in (**c**). 20 seedlings for each treatment were used. **** $p < 0.0001$. **f**, Images of median longitudinal optical sections of root meristem and mature zone stained with propidium iodide (PI) of 4d etiolated Col-0 on DMSO, 2.5 µM MBZ, and 10 µM ACC plates, 6-10 seedlings were observed for each treatment. **g-h**, Meristem length (**g**) and mature cell size (**h**) of seedlings in (**f**). 6-10 seedlings for each treatment were used. Different letters label significant different values ($p<0.0001$). One-way ANOVA and *post hoc* Tukey testing were used for statistical analysis in **g** and **h**. (Scale bar: **b**, 500 µm; **c**, 5 mm; **f**, 100 µm.). Boxplots: Whiskers: min/max values; hinges: 25th to 75th percentile; mid-line: median.

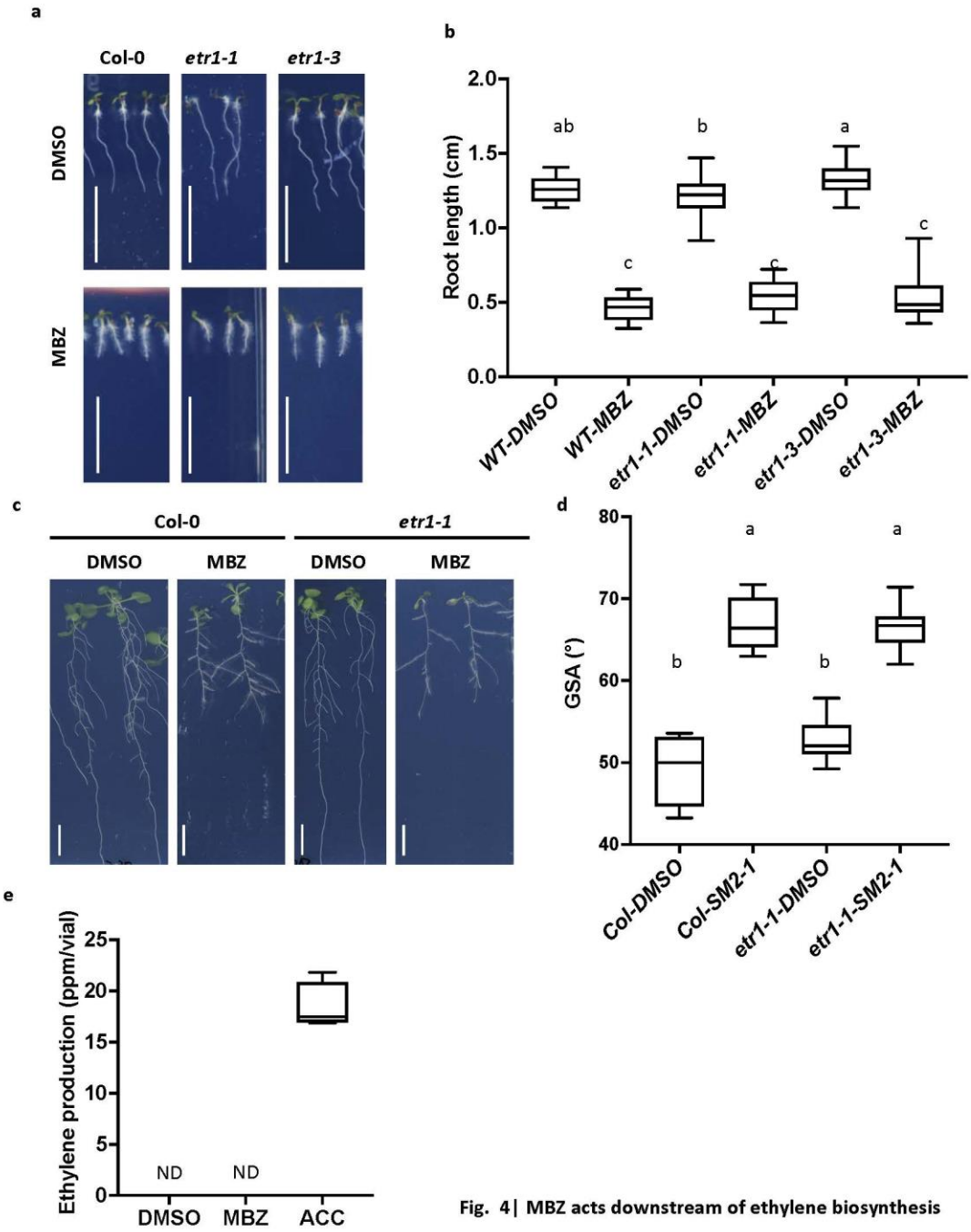

Fig. 4| MBZ acts downstream of ethylene biosynthesis

Fig. 4 | MBZ acts downstream of ethylene biosynthesis. **a**, 6d seedlings of Col-0, *etr1-1*, and *etr1-3* grown on DMSO and 1.2 μM MBZ plates. 20 seedlings were observed. **b**, Quantification of root length in (a). 20 seedlings were countified. **c**, 16d seedlings of Col-0 and *etr1-1* grown on DMSO and 1.2 μM MBZ plates. 20 seedlings were observed. **d**, Quantification of GSA in (**c**). 20 seedlings were countified. **e**,

Quantification of ethylene production by GC-MS of 4d etiolated seedlings of Col-0 in vials with DMSO, 10 µM MBZ, and 10 µM ACC medium. 100 seedlings for every vial, 4 biological replicates for each treatment, ND: not detectable. One-way ANOVA and *post hoc* Tukey testing were used for statistical analysis in b and d. Different letters label significant different values ($p<0.0001$). (Scale bar: **a**, **c**, 1 cm.) Boxplots: Whiskers: min/max values; hinges: 25th to 75th percentile; mid-line: median.

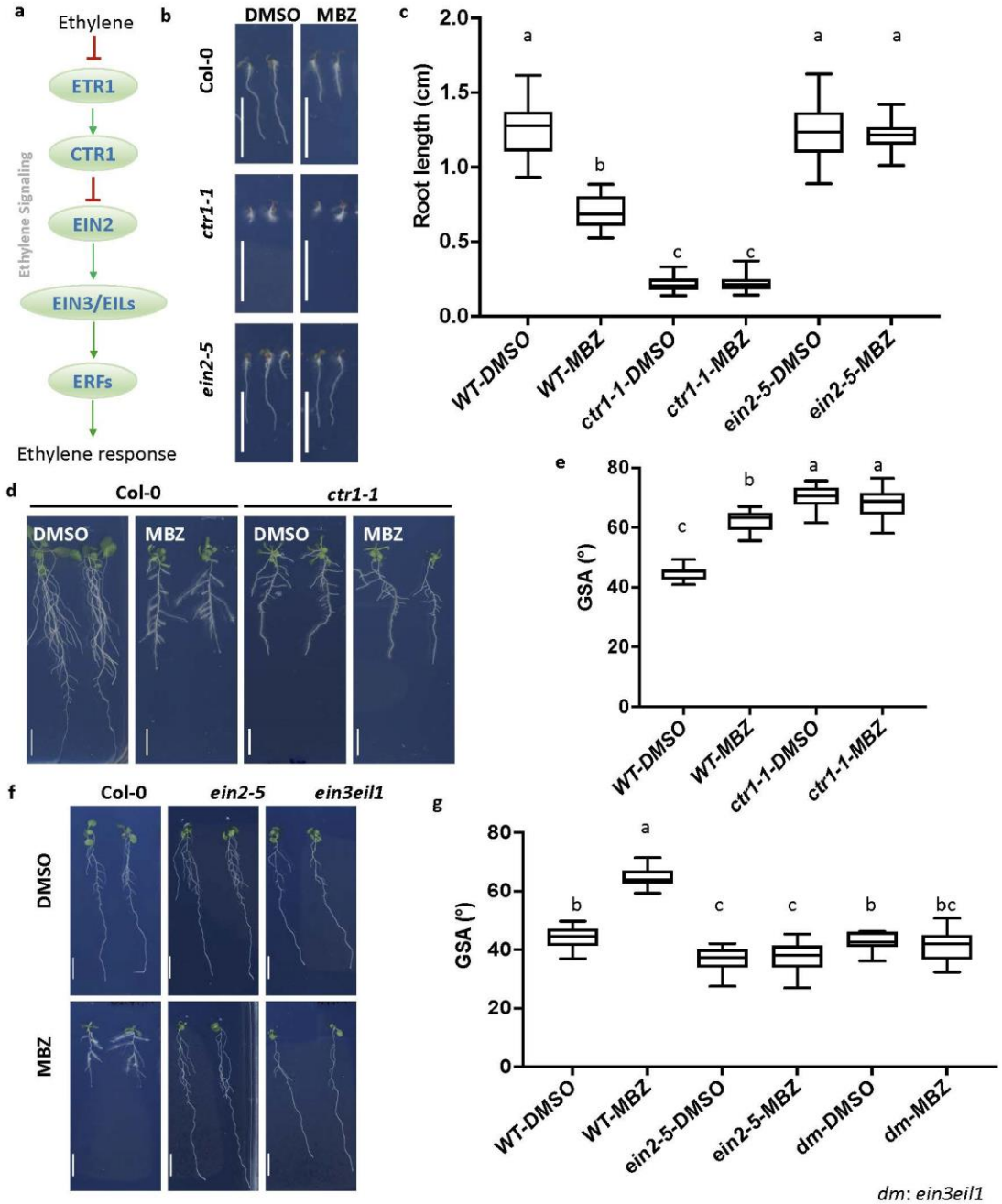

Fig. 5| MBZ targets the ethylene signaling pathway

Fig. 5 | MBZ targets the ethylene signaling pathway. **a**, Diagram of ethylene signaling pathway. **b**, 7d seedlings of Col-0, *ctr1-1*, and *ein2-5* grown on DMSO and 1.2 μM MBZ plates. **c**, Quantification of primary root length of seedlings in (**b**) 15-20 seedlings were quantified. Similar results were obtained from three biological replicates of the experiment. **d**, 19d seedlings of Col-0 and *ctr1-1* grown on DMSO and

1.3 µM MBZ plates. **e**, Quantification of GSA of seedlings in (**d**). 10 seedlings were quantified. Similar results were obtained from three biological replicates of the experiment. **f**, 16d seedlings of Col-0 and *ein2-5*, *ein3eil1* grown on DMSO and 1.3 µM MBZ plates. **g**, Quantification of GSA of seedlings in (**f**). *dm* stands for *ein3eil1* double-mutant. One-way ANOVA and *post hoc* Tukey testing were used for statistical analysis in **c**, **e**, and **g**. Different letters label significant different values ($p<0.0001$). (Scale bar: **b**, **d**, **f**, 1 cm.). Boxplots: Whiskers: min/max values; hinges: 25th to 75th percentile; mid-line: median.

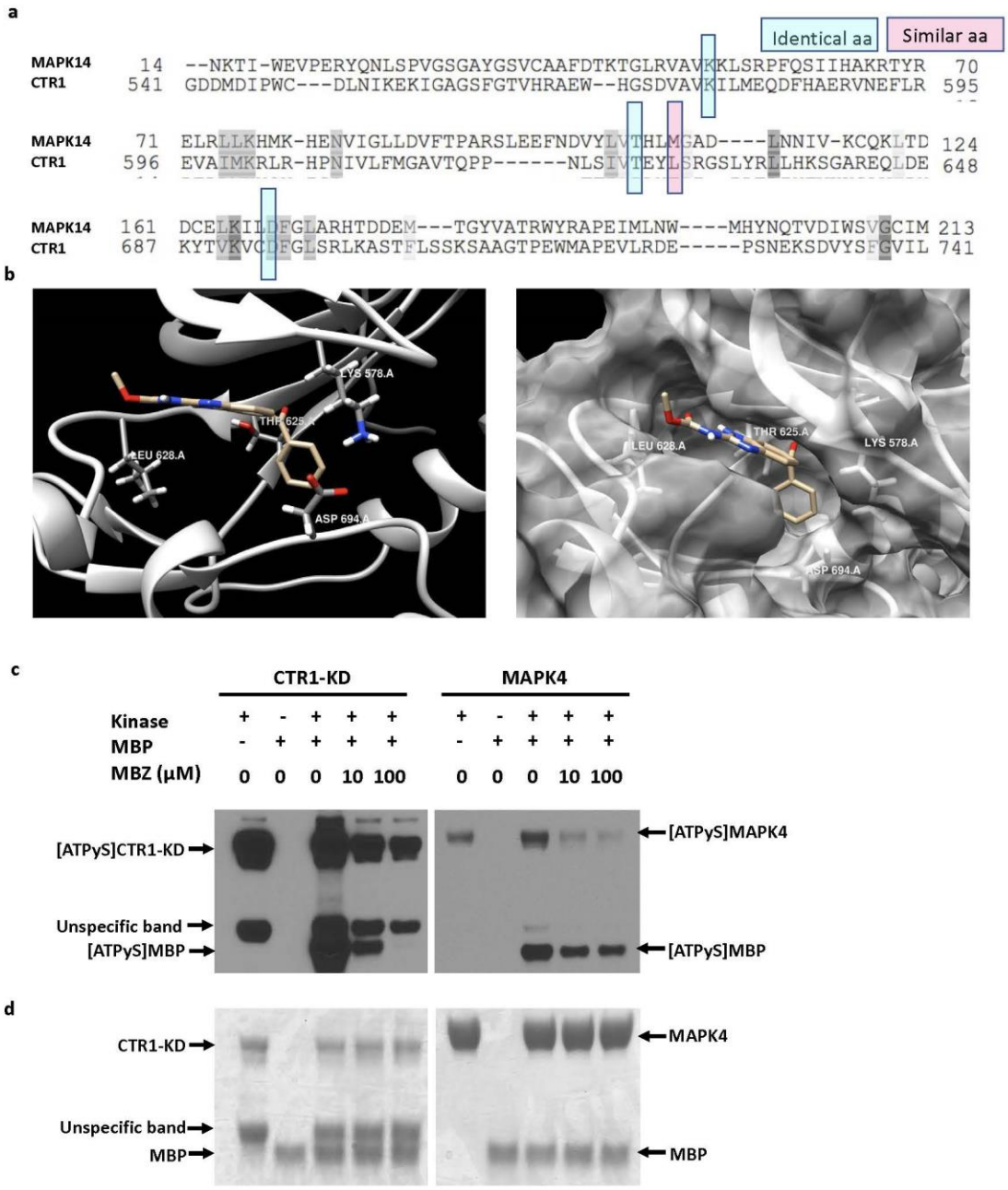

Fig. 6 | MBZ inhibits CTR1 kinase activity. **a**, Sequence alignment of *hs*MAPK14 and CTR1-KD in Arabidopsis around 4 core amino acids (Highlighted by blue and pink frames) for MBZ binding. **b**, Molecular modeling of the interaction between MBZ (coppery) and CTR1-KD (silvery). In the left panel, the key residues that contribute to the binding with CTR1-KD were highlighted. The right panel showed the surface (gray) of the catalytic pocket of CTR1-KD. **c**, Western blot using antibody of RabMAb under different concentration of MBZ treatment. Left panel: CTR1-KD; Right panel: MAPK4.

MBP is the substrate in both panels, MBZ concentration is 0, 10, and 100 μM as labeled in different reactions, [ATPyS]CTR1-KD: ATPyS binding CTR1-KD, [ATPyS]MAPK4: ATPyS binding MAPK4, MBP that obtained ATPyS from CTR1-KD or MAPK4, which is labeled as [ATPyS]MBP. **d**, Commassie blue staining of the gel shown in (**c**). CTR1: ~100 ng, MAPK4: ~1 μg. MBP: 2 μg, ATPyS: 1 mM. MBZ: 0, 10, or 100 μM. Arrows label the position of these bands on the gel.

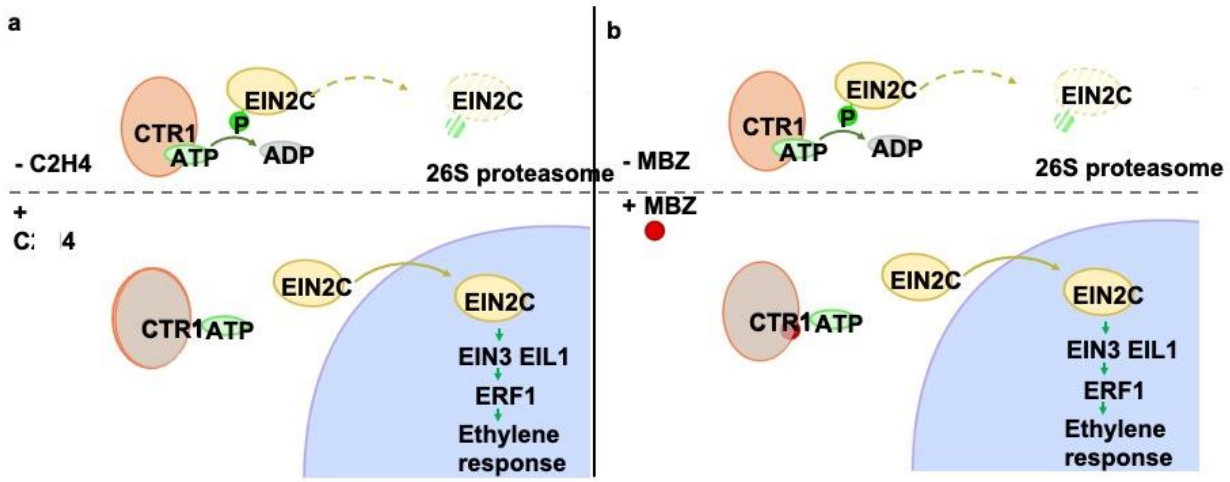

Fig. 7 | Working model for MBZ action on ethylene signaling. **a**, Ethylene suppresses CTR1 activity to promote EIN2C translocation and activates ethylene signaling. **b**, MBZ inhibits CTR1 activity by binding to its kinase domain and promotes EIN2C translocation to activate the ethylene signaling.

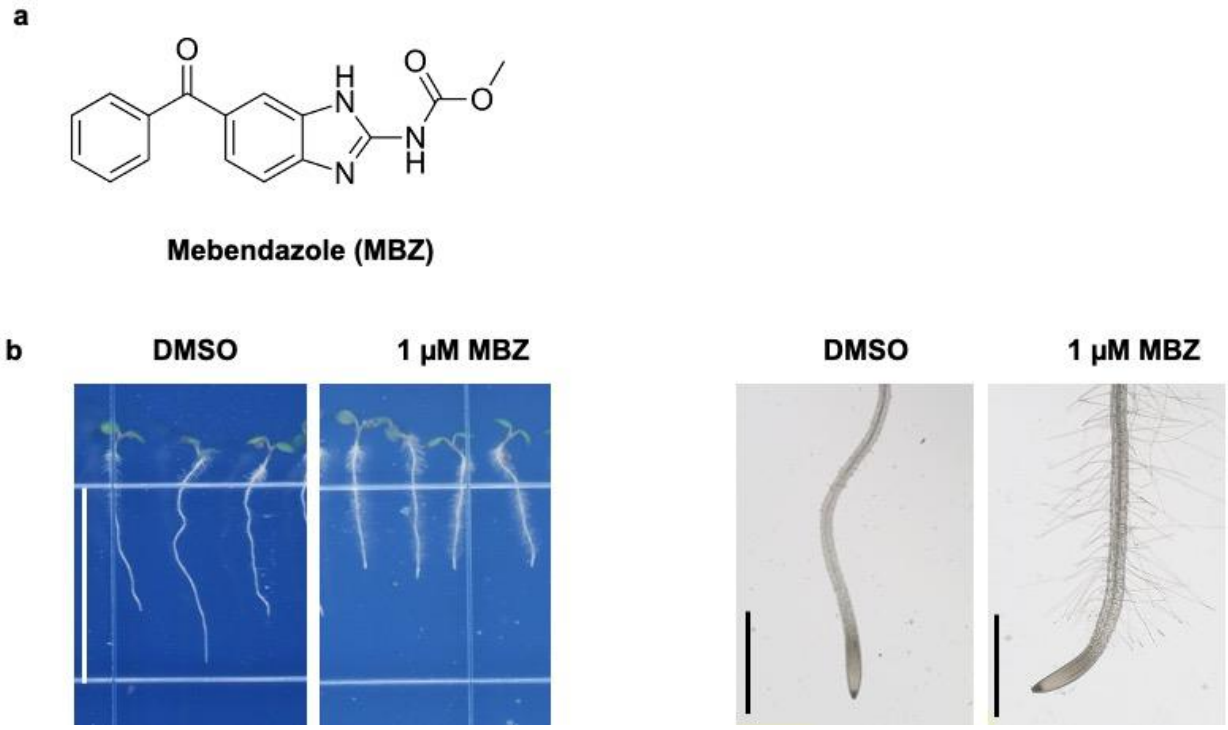

Sfig. 1 | MBZ treatment affects root growth and development. **a**, Chemical structure of MBZ. **b**, root hair phenotype of 7d seedlings on DMSO and 1 μM MBZ plates recorded by a scanner (left panel) or a microscope (right panel). 20 seedlings were observed on left panel and 10 seedlings were observed on right panel. (Scale bar: **b left panel**, 13 mm; **b right panel**, 1000μm)

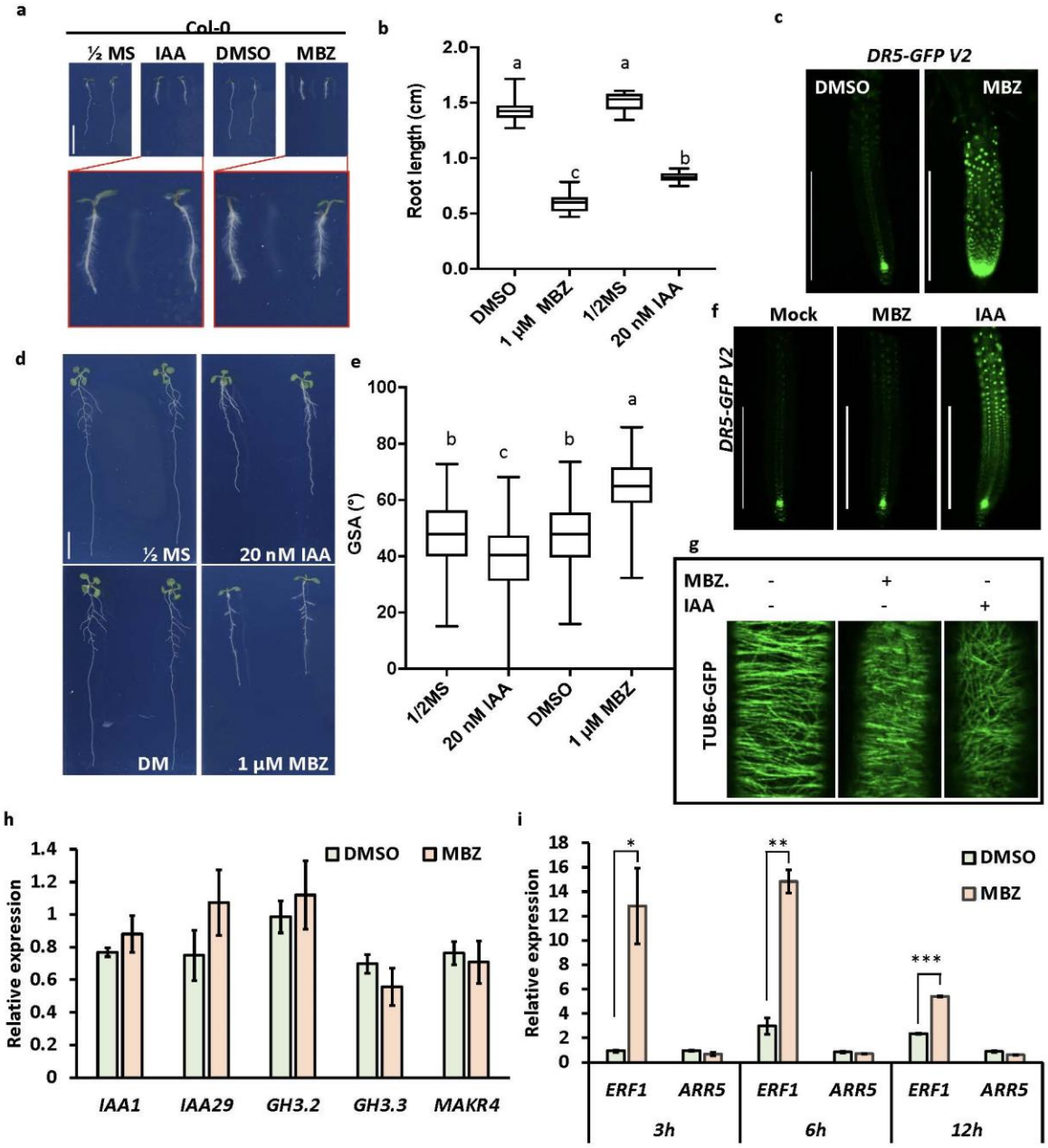

Sfig. 2 | MBZ treatment does not directly regulate auxin or cytokinin pathways. **a**, 7d Col-0 seedlings grown on ½ MS, 20 nM IAA, DMSO, and 1 μM MBZ plates. **b**, Quantification of primary root length of seedlings in (**a**). 20 seedlings were quantified for each treatment. **c**, GFP fluorescence in root tips of 7d seedlings of *DR5-GFP V2* grown on DMSO and 1 μM MBZ plates. 10 seedlings were observed. **d**, 14d Col-0 seedlings on ½ MS, 20 nM IAA, DMSO, and 1 μM MBZ plates. **e**, Quantification of GSA of

seedlings in (**d**). 20 seedlings were quantified. **f**, GFP fluorescence in root tips of 7d seedlings of *DR5-GFP V2* upon 3h treatment with H2O, 10µM MBZ, and 1 µM IAA. 6-10 seedlings were observed. **g**, GFP fluorescence in cells of root tips of 6d seedlings of *TUB6-GFP* upon 1h treatment with H2O, 50 µM MBZ, and 1 µM IAA. 6-10 seedlings were observed. **h**, Quantification of auxin marker genes expression upon 2h treatment with DMSO, and 10 µM MBZ. **i**, Quantification of ERF1 and ARR5 expression upon DMSO, and 10 µM MBZ treatment for 3 h, 6 h, and 12 h. One-way ANOVA and *post hoc* Tukey testing were used for statistical analysis in (b) and (d). Different letters label significant different values ($p<0.0001$); statistical analysis in (**h)** and (**i**) were done using unpaired, two-tailed Student's t-tests. * $p < 0.05$, ** $p < 0.01$, *** $p < 0.001$. The chart represents the mean values ± s.d. with two technical replicates. Similar results were obtained from three biological replicates of the experiment. P-values are indicated in the figure. (Scale bar: **a**, **d**, 1 cm; **c**, **f**, 500 µm). Whiskers: min/max values; hinges: 25th to 75th percentile; mid-line: median.

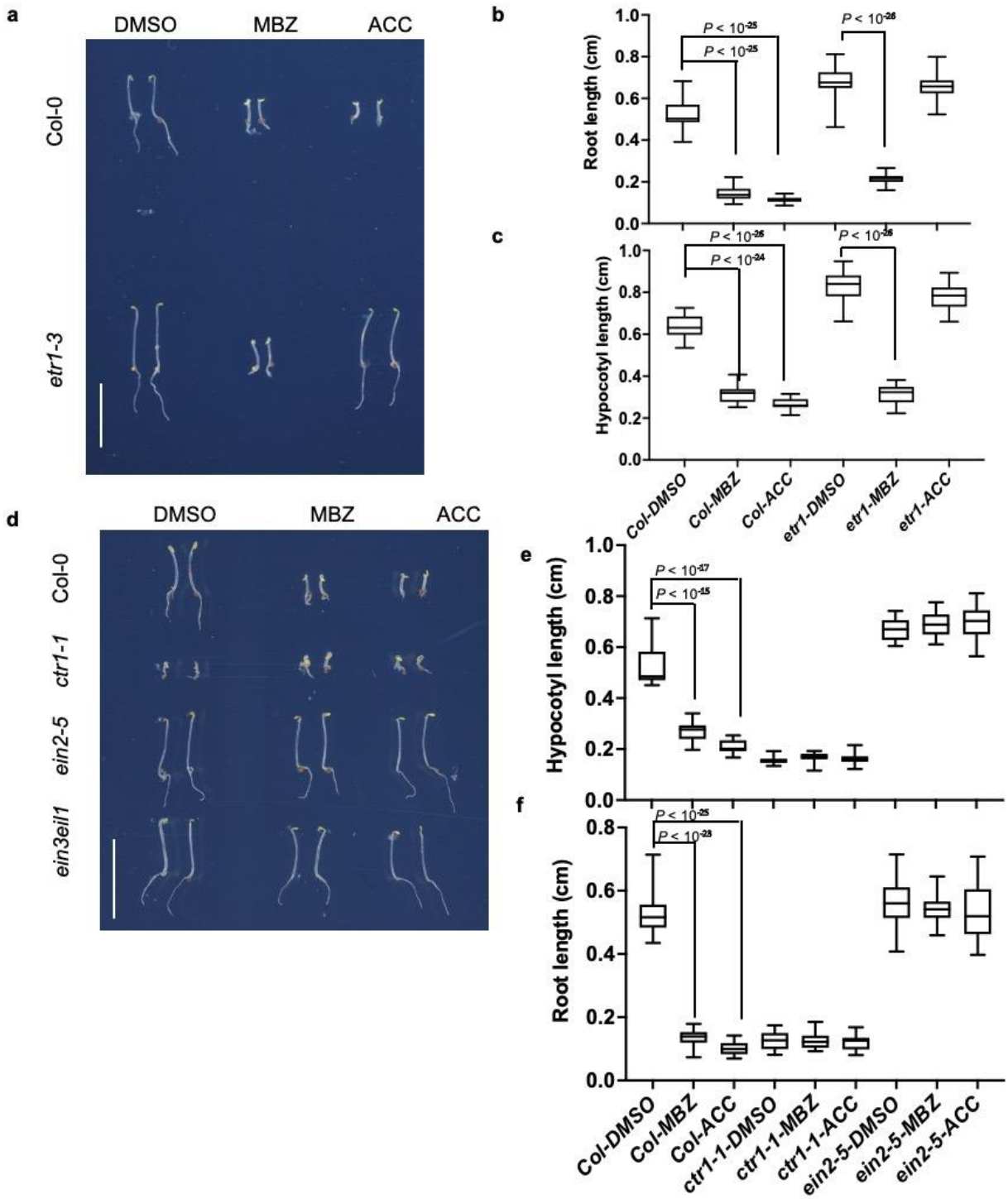

Sfig. 3 | Etiolated seedling phenotypes in mutants of the ethylene pathway. a, 4d etiolated seedlings of Col-0 and *etr1-3* grown on DMSO, 2.5 µM MBZ, and 10 µM ACC plates. **b-c**, Quantification of hypocotyl length (**b**) and root length (**c**) of seedlings in (**a**). 20 seedlings were quantified. **d**, 4d etiolated seedlings of Col-0, *ctr1-1, ein2-5*, and

ein3eil1 grown on DMSO, 2.5 µM MBZ, and 10 µM ACC plates. **e-f**, Quantification of hypocotyl length (**e**) and root length (**f**) of seedlings in **d**. 20 seedlings were quantified. Statistical analysis in **b, c** and **e, f** were done using unpaired, two-tailed Student's t-tests. P-values are indicated in the figure. (Scale bar: **a, d**, 1 cm). Whiskers: min/max values; hinges: 25th to 75th percentile; mid-line: median.

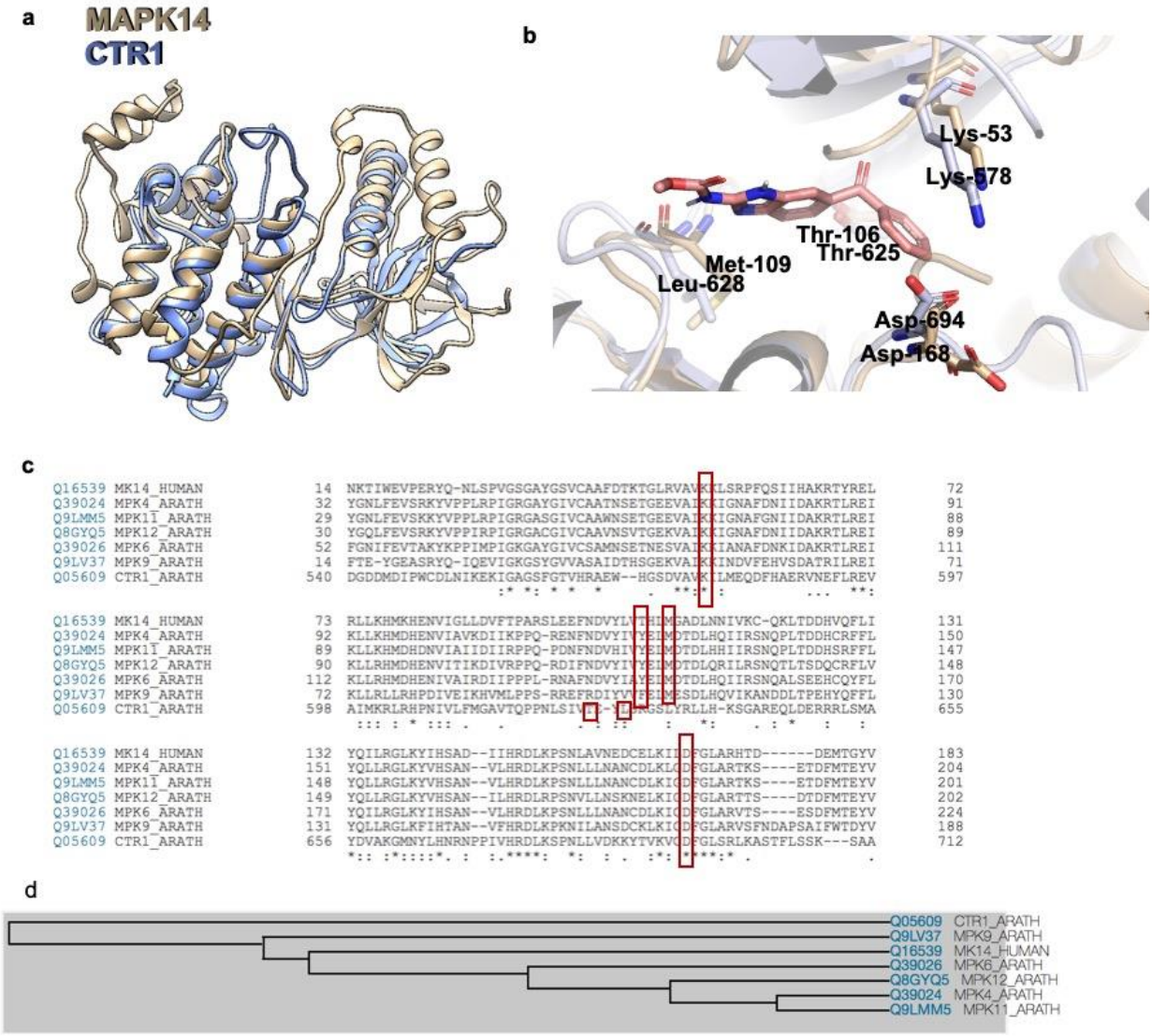

Sfig. 4 | Alignment of CTR1-KD in Arabidopsis and MAPK14 in human. **a**, The structure alignment of *hs*MAPK14 (coppery) and CTR1-KD (celeste). **b**, The protein binding sites in MAPK14 (coppery) and CTR1-KD (periwinkle) with highlighted key residues. **c**, Sequence alignment of kinase domains. Key residues in MAPK14_human and CTR1-KD in Arabidopsis are indicated by red boxes. **d**, Phylogenetic analysis of kinases aligned in (**c**).

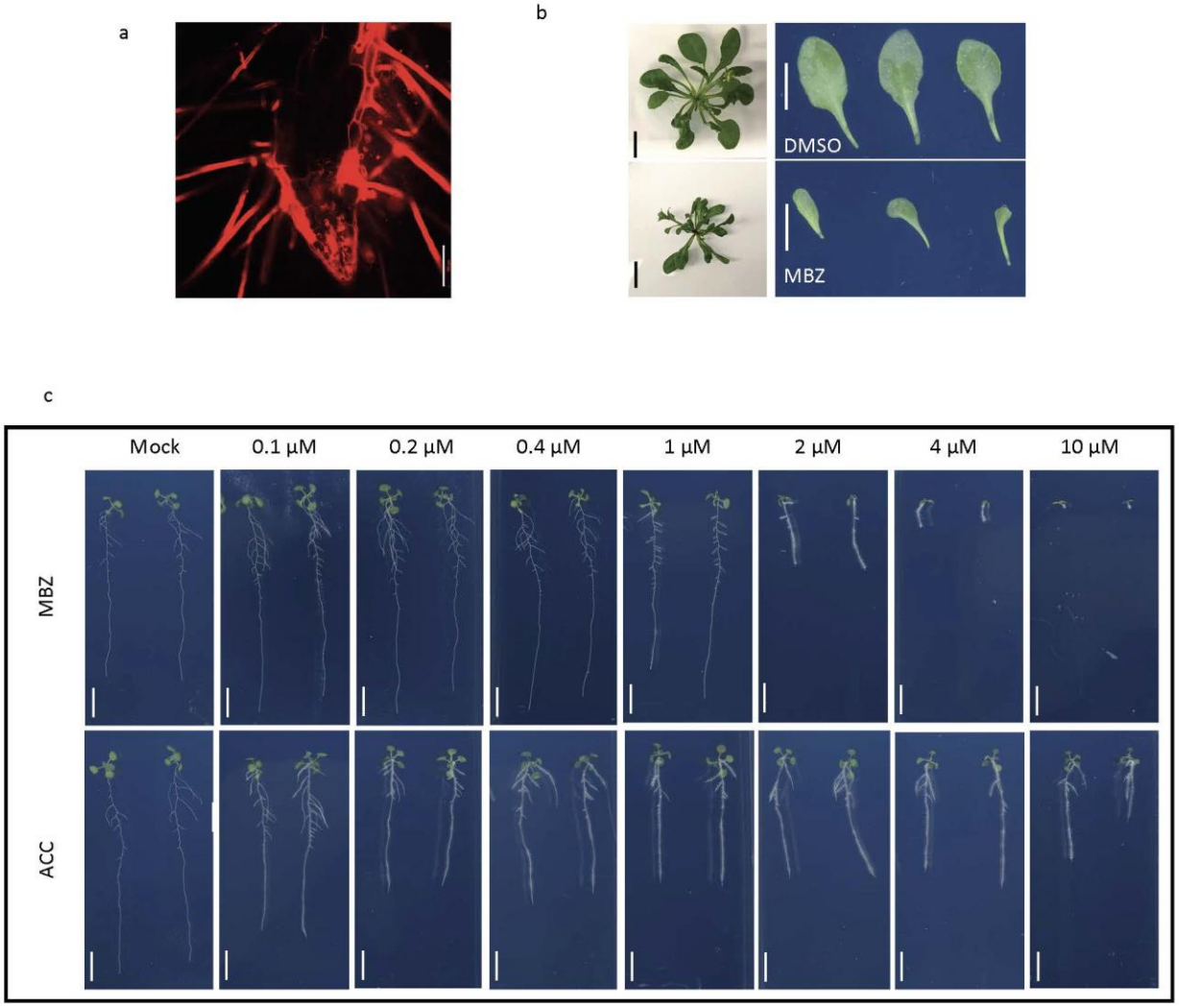

Sfig. 5 | High concentrations or long-term treatment of MBZ induce phenotypes that go beyond ethylene induced effects. **a**, Confocal microscopy images of a root meristem of 4d etiolated WT seedling grown on 10 µM MBZ plate. **b**, 38d Col-0 plants grown on DMSO and 1.2 µM MBZ plates. **c**, 14d seedlings of Col-0 grown on increasing concentrations MBZ and ACC (0.1, 0.2, 0.4, 1, 2, 4, 10 µM) 20 seedlings were observed. Similar results were obtained from three biological replicates of the experiment. (Scale bar: **a**, 100 µm, **b**, **c**, 1 cm)

JVD9H54701R-Alignment-Descriptions

Description	Scientific Name	Max Score	Total Score	Query Cover	E value	Per. ident	Acc. Len	Accession
MAP kinase 4 [Arabidopsis thaliana]	Arabidopsis thaliana	346	346	93%	3E-117	51.18	376	NP_192046.1
mitogen-activated protein kinase 4 [Arabidopsis thaliana]	Arabidopsis thaliana	346	346	93%	3E-117	51.18	376	ABR46146.1
mitogen-activated protein kinase 4 [Arabidopsis thaliana]	Arabidopsis thaliana	345	345	93%	8E-117	50.88	376	ABR46148.1
MAP kinase [Arabidopsis thaliana]	Arabidopsis thaliana	345	345	93%	9E-117	50.88	376	BAA04867.1
mitogen-activated protein kinase 4 [Arabidopsis thaliana]	Arabidopsis thaliana	344	344	93%	1E-116	50.88	376	ABR46162.1
unnamed protein product [Arabidopsis thaliana]	Arabidopsis thaliana	340	340	95%	8E-115	47.71	376	VYS62299.1
MPK5 [Arabidopsis thaliana]	Arabidopsis thaliana	339	339	95%	9E-115	47.71	376	OAO98154.1
MAP kinase 11 [Arabidopsis thaliana]	Arabidopsis thaliana	337	337	93%	6E-114	49.71	369	NP_001117210.1
unnamed protein product [Arabidopsis thaliana]	Arabidopsis thaliana	337	337	93%	6E-114	49.71	369	CAA0154293.1
MAP kinase 5 [Arabidopsis thaliana]	Arabidopsis thaliana	337	337	95%	8E-114	47.43	376	NP_567378.4
unnamed protein product [Arabidopsis thaliana]	Arabidopsis thaliana	336	336	95%	2E-113	46.84	370	CAD5324945.1
MAP kinase [Arabidopsis thaliana]	Arabidopsis thaliana	335	335	95%	2E-113	46.55	370	BAA04866.1
mitogen-activated protein kinase 3 [Arabidopsis thaliana]	Arabidopsis thaliana	335	335	95%	2E-113	46.55	370	NP_190150.1
MAP kinase [Arabidopsis thaliana]	Arabidopsis thaliana	330	330	95%	3E-111	46.57	376	BAA04868.1
mitogen-activated protein kinase 12 [Arabidopsis thaliana]	Arabidopsis thaliana	329	329	92%	9E-111	49.26	372	NP_182131.2
mitogen-activated protein kinase 12 [Arabidopsis thaliana]	Arabidopsis thaliana	330	330	92%	2E-110	49.26	406	NP_001325006.1
Mitogen-activated protein kinase 6 [Arabidopsis thaliana]	Arabidopsis thaliana	323	323	95%	2E-108	46.84	364	6DTL_A
Crystal structure of Arabidopsis thaliana MPK6 [Arabidopsis thaliana]	Arabidopsis thaliana	323	323	95%	3E-108	46.84	370	5CI6_A
unnamed protein product [Arabidopsis thaliana]	Arabidopsis thaliana	323	323	92%	3E-108	46.31	393	VYS60924.1
MAP kinase 6 [Arabidopsis thaliana]	Arabidopsis thaliana	323	323	95%	4E-108	46.84	395	NP_181907.1
MAP kinase 10 [Arabidopsis thaliana]	Arabidopsis thaliana	323	323	92%	4E-108	46.31	393	NP_191538.1
unnamed protein product [Arabidopsis thaliana]	Arabidopsis thaliana	323	323	92%	5E-108	46.31	393	CAA0387508.1
MPK10 [Arabidopsis thaliana]	Arabidopsis thaliana	323	323	92%	6E-108	46.31	393	OAP05435.1
unnamed protein product [Arabidopsis thaliana]	Arabidopsis thaliana	321	321	92%	2E-107	46.02	393	CAD5326291.1
MAP kinase [Arabidopsis thaliana]	Arabidopsis thaliana	318	318	95%	2E-106	46.29	373	CAB51417.1
Protein kinase superfamily protein [Arabidopsis thaliana]	Arabidopsis thaliana	317	317	92%	4E-106	47.79	363	NP_001030990.1
unnamed protein product [Arabidopsis thaliana]	Arabidopsis thaliana	316	316	92%	8E-106	47.79	363	CAD5312051.1
mitogen-activated protein kinase homolog 2 [Arabidopsis thaliana]	Arabidopsis thaliana	316	316	85%	2E-105	49.68	376	NP_564746.1
ATMPK1 [Arabidopsis thaliana]	Arabidopsis thaliana	315	315	93%	2E-105	46.33	370	BAA03535.1
unnamed protein product [Arabidopsis thaliana]	Arabidopsis thaliana	315	315	93%	3E-105	46.33	370	CAA0186271.1
AT1G10210 [Arabidopsis thaliana]	Arabidopsis thaliana	315	315	93%	3E-105	46.33	370	BAH19911.1
mitogen-activated protein kinase 1 [Arabidopsis thaliana]	Arabidopsis thaliana	315	315	93%	3E-105	46.33	370	NP_001031017.1
mitogen-activated protein kinase 14 [Arabidopsis thaliana]	Arabidopsis thaliana	315	315	95%	3E-105	45.04	361	NP_195363.1
ATMPK2 [Arabidopsis thaliana]	Arabidopsis thaliana	315	315	85%	4E-105	49.35	376	BAA03536.1
unnamed protein product [Arabidopsis thaliana]	Arabidopsis thaliana	313	313	95%	1E-104	45.04	361	CAA0397686.1
MPK14 [Arabidopsis thaliana]	Arabidopsis thaliana	311	311	95%	8E-104	44.76	361	OAO98488.1
MAP kinase 5-CT [Arabidopsis thaliana]	Arabidopsis thaliana	310	310	81%	9E-104	50	337	ADZ76491.1
MAP kinase 7 [Arabidopsis thaliana]	Arabidopsis thaliana	310	310	85%	2E-103	48.71	368	NP_179409.1
MPK7 [Arabidopsis thaliana]	Arabidopsis thaliana	310	310	85%	2E-103	48.71	368	OAP11026.1
MAP Kinase [Arabidopsis thaliana]	Arabidopsis thaliana	309	309	86%	4E-103	50.48	354	AAB61033.1
unnamed protein product [Arabidopsis thaliana]	Arabidopsis thaliana	310	310	91%	4E-103	48.49	389	CAD5321516.1
unnamed protein product [Arabidopsis thaliana]	Arabidopsis thaliana	309	309	85%	5E-103	48.71	368	CAA0364931.1
MAP kinase 11 [Arabidopsis thaliana]	Arabidopsis thaliana	307	307	78%	2E-102	52.08	346	NP_001322112.1
MAP kinase [Arabidopsis thaliana]	Arabidopsis thaliana	306	306	85%	1E-101	48.06	368	BAA04870.1
unnamed protein product [Arabidopsis thaliana]	Arabidopsis thaliana	310	310	86%	3E-99	48.12	716	CAD5330118.1
mitogen-activated protein kinase 12 [Arabidopsis thaliana]	Arabidopsis thaliana	297	297	80%	5E-99	51.03	324	NP_001189755.1
mitogen-activated protein kinase 16 [Arabidopsis thaliana]	Arabidopsis thaliana	287	287	91%	7E-92	42.77	567	NP_197402.1
Unknown protein [Arabidopsis thaliana]	Arabidopsis thaliana	287	287	91%	7E-92	42.77	567	AAL32607.1
unnamed protein product [Arabidopsis thaliana]	Arabidopsis thaliana	287	287	91%	9E-92	42.77	569	CAD5332107.1
MAP kinase [Arabidopsis thaliana]	Arabidopsis thaliana	276	276	75%	6E-90	50	360	BAD 95376.10
putative MAP kinase [Arabidopsis thaliana]	Arabidopsis thaliana	271	271	90%	4E-87	42.6	431	AAK62464.1
MPK15 [Arabidopsis thaliana]	Arabidopsis thaliana	274	274	92%	1E-86	41.86	575	OAP17567.1
MAP kinase 19 [Arabidopsis thaliana]	Arabidopsis thaliana	268	268	91%	3E-86	42.18	425	NP_001326968.1
MAP kinase 15 [Arabidopsis thaliana]	Arabidopsis thaliana	272	272	92%	4E-86	41.86	576	NP_565070.2
MPK8 [Arabidopsis thaliana]	Arabidopsis thaliana	269	269	92%	1E-84	42.15	588	OAP18797.1

S table 1. The list of blast hits in Arabidopsis using the MAPK14_human sequence as BLASTP.

Parsed Citations

Allen, J. J. et al. (2007) A semisynthetic epitope for kinase substrates. Nat Methods 4, 511-516, doi:10.1038/nmeth1048
Google Scholar: Author Only Title Only Author and Title

Alonso, J. M., Hirayama, T., Roman, G., Nourizadeh, S. & Ecker, J. R. (1999) EIN2, a bifunctional transducer of ethylene and stress responses in Arabidopsis. Science 284, 2148-2152, doi:10.1126/science.284.5423.2148
Google Scholar: Author Only Title Only Author and Title

An, F. et al. (2010) Ethylene-induced stabilization of ETHYLENE INSENSITIVE3 and EIN3-LIKE1 is mediated by proteasomal degradation of EIN3 binding F-box 1 and 2 that requires EIN2 in Arabidopsis. Plant Cell 22, 2384-2401, doi:10.1105/tpc.110.076588
Google Scholar: Author Only Title Only Author and Title

Ariey-Bonnet, J. et al. (2020) In silico molecular target prediction unveils mebendazole as a potent MAPK14 inhibitor. Mol Oncol 14, 3083-3099, doi:10.1002/1878-0261.12810
Google Scholar: Author Only Title Only Author and Title

Berardini, T. Z. et al. (2015) The Arabidopsis information resource: Making and mining the "gold standard" annotated reference plant genome. Genesis 53, 474-485, doi:10.1002/dvg.22877
Google Scholar: Author Only Title Only Author and Title

Chang, C., Kwok, S. F., Bleecker, A. B. & Meyerowitz, E. M. (1993) Arabidopsis ethylene-response gene ETR1: similarity of product to two-component regulators. Science 262, 539-544, doi:10.1126/science.8211181
Google Scholar: Author Only Title Only Author and Title

Chang, K. N. et al. (2013) Temporal transcriptional response to ethylene gas drives growth hormone cross-regulation in Arabidopsis. Elife 2, e00675, doi:10.7554/eLife.00675
Google Scholar: Author Only Title Only Author and Title

Chao, Q. et al. (1997) Activation of the ethylene gas response pathway in Arabidopsis by the nuclear protein ETHYLENE-INSENSITIVE3 and related proteins. Cell 89, 1133-1144, doi:10.1016/s0092-8674(00)80300-1
Google Scholar: Author Only Title Only Author and Title

Chen, X. et al. (2014) Inhibition of cell expansion by rapid ABP1-mediated auxin effect on microtubules. Nature 516, 90-93, doi:10.1038/nature13889
Google Scholar: Author Only Title Only Author and Title

De Cnodder, T., Vissenberg, K., Van Der Straeten, D. & Verbelen, J. P. (2005) Regulation of cell length in the Arabidopsis thaliana root by the ethylene precursor 1-aminocyclopropane- 1-carboxylic acid: a matter of apoplastic reactions. New Phytol 168, 541-550, doi:10.1111/j.1469-8137.2005.01540.x
Google Scholar: Author Only Title Only Author and Title

Dobin, A. et al. (2013) STAR: ultrafast universal RNA-seq aligner. Bioinformatics 29, 15-21, doi:10.1093/bioinformatics/bts635
Google Scholar: Author Only Title Only Author and Title

Feng, Y. et al. (2017) Ethylene promotes root hair growth through coordinated EIN3/EIL1 and RHD6/RSL1 activity in Arabidopsis. Proc Natl Acad Sci U S A 114, 13834-13839, doi:10.1073/pnas.1711723115
Google Scholar: Author Only Title Only Author and Title

Guo, H. & Ecker, J. R. (2004) The ethylene signaling pathway: new insights. Curr Opin Plant Biol 7, 40-49, doi:10.1016/j.pbi.2003.11.011
Google Scholar: Author Only Title Only Author and Title

Guzman, P. & Ecker, J. R. (1990) Exploiting the triple response of Arabidopsis to identify ethylene-related mutants. Plant Cell 2, 513-523, doi:10.1105/tpc.2.6.513
Google Scholar: Author Only Title Only Author and Title

He, W. et al. (2011) A small-molecule screen identifies L-kynurenine as a competitive inhibitor of TAA1/TAR activity in ethylene-directed auxin biosynthesis and root growth in Arabidopsis. Plant Cell 23, 3944-3960, doi:10.1105/tpc.111.089029
Google Scholar: Author Only Title Only Author and Title

Hua, J. et al. (1998) EIN4 and ERS2 are members of the putative ethylene receptor gene family in Arabidopsis. Plant Cell 10, 1321-1332, doi:10.1105/tpc.10.8.1321
Google Scholar: Author Only Title Only Author and Title

Ju, C. et al. (2012) CTR1 phosphorylates the central regulator EIN2 to control ethylene hormone signaling from the ER membrane to the nucleus in Arabidopsis. Proc Natl Acad Sci U S A 109, 19486-19491, doi:10.1073/pnas.1214848109
Google Scholar: Author Only Title Only Author and Title

Ju, C. et al. (2015) Conservation of ethylene as a plant hormone over 450 million years of evolution. Nat Plants 1, 14004,

doi:10.1038/nplants.2014.4
Google Scholar: Author Only Title Only Author and Title

Kieber, J. J., Rothenberg, M., Roman, G., Feldmann, K. A. & Ecker, J. (1993) R. CTR1, a negative regulator of the ethylene response pathway in Arabidopsis, encodes a member of the raf family of protein kinases. Cell 72, 427-441, doi:10.1016/0092-8674(93)90119-b
Google Scholar: Author Only Title Only Author and Title

Le, J., Vandenbussche, F., Van Der Straeten, D. & Verbelen, J. P. (2001) In the early response of Arabidopsis roots to ethylene, cell elongation is up- and down-regulated and uncoupled from differentiation. Plant Physiol 125, 519-522, doi:10.1104/pp.125.2.519
Google Scholar: Author Only Title Only Author and Title

Leinonen, R., Sugawara, H., Shumway, M. (2011) & International Nucleotide Sequence Database, C. The sequence read archive. Nucleic Acids Res 39, D19-21, doi:10.1093/nar/gkq1019
Google Scholar: Author Only Title Only Author and Title

Li, B. et al. (2019) GSNOR provides plant tolerance to iron toxicity via preventing iron-dependent nitrosative and oxidative cytotoxicity. Nat Commun 10, 3896, doi:10.1038/s41467-019-11892-5
Google Scholar: Author Only Title Only Author and Title

Liao, C. Y. et al. (2015) Reporters for sensitive and quantitative measurement of auxin response. Nat Methods 12, 207-210, 202 p following 210, doi:10.1038/nmeth.3279
Google Scholar: Author Only Title Only Author and Title

Lynch, J. P. (2021). Harnessing root architecture to address global challenges. Plant J, doi:10.1111/tpj.15560
Google Scholar: Author Only Title Only Author and Title

Lynch, J. P. (2019). Root phenotypes for improved nutrient capture: an underexploited opportunity for global agriculture. New Phytol 223, 548-564, doi:10.1111/nph.15738
Google Scholar: Author Only Title Only Author and Title

Mayerhofer, H., Mueller-Dieckmann, C. & Mueller-Dieckmann, J. (2011) Cloning, expression, purification and preliminary X-ray analysis of the protein kinase domain of constitutive triple response 1 (CTR1) from Arabidopsis thaliana. Acta Crystallogr Sect F Struct Biol Cryst Commun 67, 117-120, doi:10.1107/S1744309110047640
Google Scholar: Author Only Title Only Author and Title

Mayerhofer, H., Panneerselvam, S. & Mueller-Dieckmann, J. (2012) Protein kinase domain of CTR1 from Arabidopsis thaliana promotes ethylene receptor cross talk. J Mol Biol 415, 768-779, doi:10.1016/j.jmb.2011.11.046
Google Scholar: Author Only Title Only Author and Title

Mou, W. et al. (2020) Ethylene-independent signaling by the ethylene precursor ACC in Arabidopsis ovular pollen tube attraction. Nat Commun 11, 4082, doi:10.1038/s41467-020-17819-9
Google Scholar: Author Only Title Only Author and Title

Muller, M. & Munne-Bosch, S. (2015) Ethylene Response Factors: A Key Regulatory Hub in Hormone and Stress Signaling. Plant Physiol 169, 32-41, doi:10.1104/pp.15.00677
Google Scholar: Author Only Title Only Author and Title

Nakamura, M., Naoi, K., Shoji, T. & Hashimoto, T. (2004) Low concentrations of propyzamide and oryzalin alter microtubule dynamics in Arabidopsis epidermal cells. Plant Cell Physiol 45, 1330-1334, doi:10.1093/pcp/pch300
Google Scholar: Author Only Title Only Author and Title

Negi, S., Ivanchenko, M. G. & Muday, G. K. (2008) Ethylene regulates lateral root formation and auxin transport in Arabidopsis thaliana. Plant J 55, 175-187, doi:10.1111/j.1365-313X.2008.03495.x
Google Scholar: Author Only Title Only Author and Title

Ogura, T. et al. (2019) Root System Depth in Arabidopsis Is Shaped by EXOCYST70A3 via the Dynamic Modulation of Auxin Transport. Cell 178, 400-412 e416, doi:10.1016/j.cell.2019.06.021
Google Scholar: Author Only Title Only Author and Title

Ogura, T., Goeschl, C. & Busch, W. (2022) A Multiplexed, Time-Resolved Assay of Root Gravitropic Bending on Agar Plates. Methods Mol Biol 2368, 61-70, doi:10.1007/978-1-0716-1677-2_4
Google Scholar: Author Only Title Only Author and Title

Pattyn, J., Vaughan-Hirsch, J. & Van de Poel, B. (2021) The regulation of ethylene biosynthesis: a complex multilevel control circuitry. New Phytol 229, 770-782, doi:10.1111/nph.16873
Google Scholar: Author Only Title Only Author and Title

Poirier, V., Roumet, C. & Munson, A. D. (2018). The root of the matter: Linking root traits and soil organic matter stabilization processes. Soil Biology and Biochemistry 120, 246-259, doi:https://doi.org/10.1016/j.soilbio.2018.02.016

Google Scholar: Author Only Title Only Author and Title

Qiao, H. et al. (2012) Processing and subcellular trafficking of ER-tethered EIN2 control response to ethylene gas. Science 338, 390-393, doi:10.1126/science.1225974
Google Scholar: Author Only Title Only Author and Title

Ristova, D., Giovannetti, M., Metesch, K. & Busch, W. (2018) Natural genetic variation shapes root system responses to phytohormones in Arabidopsis. Plant J 96, 468-481, doi:10.1111/tpj.14034
Google Scholar: Author Only Title Only Author and Title

Robinson, M. D., McCarthy, D. J. & Smyth, G. K. (2010) edgeR: a Bioconductor package for differential expression analysis of digital gene expression data. Bioinformatics 26, 139-140, doi:10.1093/bioinformatics/btp616
Google Scholar: Author Only Title Only Author and Title

Rosquete, M. R. et al. (2013).An auxin transport mechanism restricts positive orthogravitropism in lateral roots. Curr Biol 23, 817-822, doi:10.1016/j.cub.2013.03.064
Google Scholar: Author Only Title Only Author and Title

Roychoudhry, S., Del Bianco, M., Kieffer, M. & Kepinski, S. (2013). Auxin controls gravitropic setpoint angle in higher plant lateral branches. Curr Biol 23, 1497-1504, doi:10.1016/j.cub.2013.06.034
Google Scholar: Author Only Title Only Author and Title

Sakai, H. et al. ETR2 is an ETR1-like gene involved in ethylene signaling in Arabidopsis (1998) Proc Natl Acad Sci U S A 95, 5812-5817, doi:10.1073/pnas.95.10.5812
Google Scholar: Author Only Title Only Author and Title

Sun, X. et al. (2017) Pyrazinamide and derivatives block ethylene biosynthesis by inhibiting ACC oxidase. Nat Commun 8, 15758, doi:10.1038/ncomms15758
Google Scholar: Author Only Title Only Author and Title

Uga, Y. et al. (2013).Control of root system architecture by DEEPER ROOTING 1 increases rice yield under drought conditions. Nat Genet 45, 1097-1102, doi:10.1038/ng.2725
Google Scholar: Author Only Title Only Author and Title

Vaseva, II et al. (2018) The plant hormone ethylene restricts Arabidopsis growth via the epidermis. Proc Natl Acad Sci U S A 115, E4130-E4139, doi:10.1073/pnas.1717649115
Google Scholar: Author Only Title Only Author and Title

Waidmann, S. et al. (2019) Cytokinin functions as an asymmetric and anti-gravitropic signal in lateral roots. Nat Commun 10, 3540, doi:10.1038/s41467-019-11483-4
Google Scholar: Author Only Title Only Author and Title

Wen, X. et al. (2012) Activation of ethylene signaling is mediated by nuclear translocation of the cleaved EIN2 carboxyl terminus. Cell Res 22, 1613-1616, doi:10.1038/cr.2012.145
Google Scholar: Author Only Title Only Author and Title

Xiao, G. & Zhang, Y. (2020). Adaptive Growth: Shaping Auxin-Mediated Root System Architecture. Trends Plant Sci 25, 121-123, doi:10.1016/j.tplants.2019.12.001
Google Scholar: Author Only Title Only Author and Title

Yang, S F & Hoffman, N. E. 1984) Ethylene Biosynthesis and its Regulation in Higher Plants. Annual Review of Plant Physiology 35, 155-189, doi:10.1146/annurev.pp.35.060184.001103
Google Scholar: Author Only Title Only Author and Title

Zhu, Y. et al. (2019) A phenotype-directed chemical screen identifies ponalrestat as an inhibitor of the plant flavin monooxygenase YUCCA in auxin biosynthesis. J Biol Chem 294, 19923-19933, doi:10.1074/jbc.RA119.010480
Google Scholar: Author Only Title Only Author and Title